

1 **Response to reviews**

2 The authors are grateful for all the helpful comments of the two anonymous reviewers, which have  
3 resulted in an improved manuscript. Substantial changes have been made to the original  
4 manuscript, including the following: (1) the removal of convexity from the testing procedure; (2)  
5 the implementation of the Benjamini and Hochberg procedure to control the false discovery rate  
6 of the geometric test; (3) the addition of an in-depth discussion explaining the fundamental  
7 differences between the geometric and areawise tests; (4) the inclusion of sensitivity studies in  
8 Sect. 5; (5) the addition of a brief discussion of how the results of the methods would change if  
9 another analyzing wavelet was used; (6) the addition of two figures, which better illustrate the  
10 methods. Changes in nomenclature and mathematical notation have also been made. Discussions  
11 of figures have been improved to facilitate the interpretation of results. Finally, results from other  
12 climate studies are better integrated with the results obtained using the proposed methods,  
13 providing motivation for the application of the methods in future studies.  
14 What follows is a point-by-point response to the two anonymous reviewers. Reviewer comments  
15 have been reproduced in bold text and our responses are in plain text. All references to line and  
16 page numbers pertain to the original manuscript.

17  
18  
19 **Reviewer 1**

20  
21 **The present study will be an important addition to the significance testing of wavelet spectra.**  
22 **It provides what may be a useful alternative to the existing “areawise” test and also provides**  
23 **a new topological approach. Before publication, however, several unresolved issues need to**  
24 **be addressed. First, the consequences of a major assumption made in the method need to be**  
25 **discussed. Second, the authors justify the need for this test by the “multiple testing problem”**  
26 **but then they do not show how their test improves upon the pointwise test that was the**  
27 **motivating issue. Third, they also need to improve the figures and their discussion of them.**  
28 **Fourth, the authors should justify their climate examples that use short segments from**  
29 **available long climate series or use longer ones. Additionally, many minor issues of clarity**  
30 **need to be addressed. Putting some of this work in the context of other climate studies would**  
31 **also be helpful and increase the importance of this study for climate science.**

32  
33 We are grateful for these thoughtful comments, which are addressed in detail in the responses to  
34 the general and specific comments listed below.

35  
36 **General comments**

37 **I. The proposed geometric test suffers from a binary decision of a pointwise threshold**  
38 **“significance” or not. The authors showed some sensitivity to that threshold. The authors**

1 **should at least discuss an alternative test, very similar in spirit, which does not use binary**  
2 **assessments: the false discovery rate (Wilks 2006).**

3  
4 In the summary section, a discussion has been added that offers a potential other method for  
5 minimizing the number of false positive results. The discussion includes the following paragraph:  
6 “One disadvantage of the geometric and areawise tests is that they require a binary decision in  
7 which pointwise and geometric significance levels must be chosen. The binary decision can be  
8 circumvented by applying a  $p$ -value adjustment procedure to the wavelet power coefficients  
9 directly. For example, one could apply the Benjamini and Hochberg (1995) procedure to the  
10 wavelet power coefficients or a modified version of the procedure developed by Benjamini and  
11 Yekutieli (2002), which is valid for any dependency structure among the local test statistics. The  
12 latter procedure would seem most appropriate given the autocorrelation structure of wavelet power  
13 coefficients; however, it is noted that the procedure has considerably less statistical power than the  
14 original procedure valid for independent local test statistics, though Wilks (2006) found the  
15 Benjamini and Hochberg (1995) procedure to remain powerful even when the assumption of  
16 independence is violated.”

17  
18 **II. The authors need to justify the “coordinate system” being scale index. The width of the**  
19 **analyzing wavelet changes as a function of scale. I expect that the significance of a wide patch**  
20 **at a small scale to be different from a wide patch at a large scale. The calculation may be**  
21 **“simpler”, but it could also be the wrong area to assess. This is my single biggest concern**  
22 **with this testing procedure. The authors need to show that using the actual coordination**  
23 **system would result in the same distribution of chi.**

24  
25 To remove any ambiguity, we have chosen to use the actual coordinate system in the testing  
26 procedure, though it was found that using the other coordinate system did not change the geometric  
27 significance of patches.

28  
29 **III. The areawise test based on the reproducing kernel of Maraun et al. 2007 is strictly limited**  
30 **to Gaussian white noise. The present authors are also making use of the reproducing kernel**  
31 **in their equation 10 and subsequent steps. a) How does what should be a changing kernel as**  
32 **a function of the noise alter the effectiveness or sensitivity of both the areawise and this**  
33 **geometric test? This is particularly relevant for the comparison testing in Section 4.2 and**  
34 **may be an additional strength of the geometric test if it is less sensitive to the form of the**  
35 **noise and the error in the kernel.**

36  
37 Maraun et al. (2007) found that the areawise test was insensitive to the form of noise. In particular,  
38 the areawise test does not depend on the choice of lag-1 autocorrelation correlation coefficient for  
39 red-noise processes. This independence to the form of noise is supported by the comparison of the  
40 areawise and geometric tests for different lag-1 autocorrelation coefficients, which has now been  
41 added in Sect. 4 and is also now shown in Fig. 4 (now Fig. 6).

42  
43 **b) The comparison testing of Section 4.2 needs to be performed on different AR1 noises from**  
44 **an AR1 parameter of 0 to nearly 1. The reproducing kernel of Maraun et al. 2007 becomes**

1 **less and less relevant as the auto-correlation increases, but the area of random significant**  
2 **patches could continue to grow as the AR1 parameter is increased.**

3  
4 The comparison between the two tests for different AR1 parameters has been added to Sect. 4. It  
5 turns out that the area of random significance patches is weakly dependent on the AR1 parameter.  
6

#### 7 **IV. The authors need to better motivate including convexity in the testing procedure.**

8  
9 After further investigation, the inclusion of convexity was found to only play a minor role in the  
10 results of the testing procedure. On the other hand, convexity can explain the differences between  
11 the areawise and geometric tests. Thus, convexity has been removed from testing procedure but is  
12 included in the discussion of why the tests differ. It is noted that the removal of convexity makes  
13 the geometric test generally less conservative than the areawise test, a problem that was remedied  
14 by controlling the false discovery rate using the Benjamini and Hochberg (1995) procedure. See  
15 the response to comment 21 for details.  
16

#### 17 **V. The present method still seems to suffer from the multiple testing problem. If I have 20** 18 **patches and find 2 that are geometrically significant, how is the probability that both were** 19 **still the result of the noise process addressed?**

20  
21 Indeed, the present method still suffers from the multiple testing problem. The multiple testing  
22 problem has been resolved through the application of the Benjamini and Hochberg (1995) method.  
23 A new section (now Sect. 4.2) has been added, which describes the procedure and the procedure  
24 is used throughout the paper to control the false discovery at the 0.05 level. See response to  
25 comment 23 for details.  
26

#### 27 **VI. Recent work (Hanna et al. 2014) claimed to detect a trend in the variance of the NAO.** 28 **The present study's wavelet analysis of the NAO and new statistical significance testing** 29 **procedure would be the ideal place to evaluate that claim. The authors should comment on** 30 **any significant changes in variance detected.**

31  
32 A comment about this study was added on page 1343 line 25 to put the results of the method in  
33 the context of climate science.  
34

#### 35 **VII. Can the authors provide some computer code or pseudo-code for how to implement** 36 **their procedure?**

37  
38 We would be pleased to make Matlab code available and will provide such in the journal's  
39 supplementary information if this is permitted or by request to the first author.  
40

#### 41 **Specific comments**

42  
43 **1. pg 1332 line 19. The introductory juxtaposition of "random" and "meaningful" does not**  
44 **make sense. I think what is meant is stochastic or deterministic. Random structures are**  
45 **meaningful. The assessment is essential to understand the predictability of the system.**  
46

1 The words “random” and “meaningful” have been replaced by “stochastic” and deterministic” on  
2 page 1332 line 19.

3 **2. line 1333 line 15. Some reference for the “climate science” procedure of comparing spectra**  
4 **to red noise should be given.**

5  
6 A reference (Hasselmann, 1976) is now given on page 1333 line 15.

7  
8 **3. pg 1334 line 5. The use of the phraseology “Moreover, the areawise,...” is confusing. The**  
9 **term areawise has not been introduced or defined.**

10 The term areawise in the context of significance testing has now been introduced on page 1333  
11 line 3 in the introduction section.

12  
13 **4. pg 1334 line 13. “holes” has not been defined. The meaning here is unclear. Please clarify.**

14  
15 An informal definition of a hole has been inserted on page 1334 line 13 and the reader is now  
16 referred to Sect. 5 for a more formal definition of a hole.

17  
18 **5. pg 1335 line 20. What is meant by “Another interesting feature emerges: periods of**  
19 **reduced pointwise significance surrounded by regions of pointwise significance.” I don’t see**  
20 **anything like this indicated on the figure.**

21  
22 The phraseology has been changed on page 1335 line 20 to clarify the feature of interest. Also,  
23 included on the corresponding figure is a label to help guide the reader.

24  
25 **6. pg 1336 line 4, “reproducing kernel” should be defined before its importance is discussed.**

26  
27 The importance of the reproducing kernel is now discussed on page 1336 line 4.

28  
29 **7. pg 1336 lines 8 and 9. The structure of the vaguely referenced equation relating the**  
30 **reproducing kernel to the correlation between wavelet coefficients is important to the**  
31 **argument and explanation here. The equation should be reproduced and then cited.**

32  
33 The equation for the correlation structure of wavelet coefficients has now been reproduced and  
34 cited on page 1336 line 8.

35  
36 **8. pg 1336 line 9. Is the area “given by” the reproducing kernel, or is the typical patch area**  
37 **the area of the reproducing kernel?**

38  
39 The phraseology on page 1336 line 9 has been changed to “the typical patch area is the area of the  
40 reproducing kernel.”

41  
42 **9. pg 1336 line 9 and following. What is meant precisely by area in this context should be**  
43 **defined. Particularly because the subsequent area of the geometric test is different.**

44

1 A sentence was added to page 1336 line 15 to clarify what the area is in the context of the areawise  
2 test. Another clarifying sentence was added on page 1336 line 20 to help distinguish between the  
3 area used in the geometric and areawise tests.

4  
5 **10. pg 1336 line 16. Is the test for “any” reproducing kernel or the reproducing kernel  
6 corresponding to the analyzing wavelet?**

7  
8 The test should be performed with the reproducing kernel corresponding to the analyzing wavelet  
9 and the wording has been changed on page 1336 line 16 to reflect that.

10  
11 **11. page 1336 line 20. One is not assessing the significance of the wavelet coefficients. One is  
12 assessing the wavelet spectrum or the coefficients squared.**

13  
14 “Wavelet coefficients” have been changed to “wavelet power coefficients” on page 1336 line 20

15  
16 **12. page 1337 line 4-10. The discussion of the illustration needs improvement. Please provide  
17 the reader some specific examples so that they know what they are looking at. At what time  
18 and scale are some of these features seen? Why is Figure 1 plotted so differently from Figure  
19 2? What are the red noise parameters being used?**

20  
21 Fig. 1 and Fig. 2. (now Figs. 3 and 4) are now plotted identically, with light gray shading  
22 representing those 5% pointwise significance patches that are geometrically significant and dark  
23 gray shading indicating those 1% pointwise significance patches that are geometrically significant.  
24 A more detailed discussion has been added to page 1337 line 4 to highlight some specific features.

25  
26 **13. equation 7. It may seem pedantic, but please include how this discrete equation 7 follows  
27 from Green’s theorem, which applies to integrals (perhaps in a small appendix or provide a  
28 reference).**

29  
30 A new appendix (Appendix C) has been added to the manuscript where the derivation of Green’s  
31 theorem for a polygon is given. Equation (7) is now also cited.

32  
33 **14. equation 7. The variable  $n$  is not defined.**

34  
35  $n$ , which has been changed to  $m$ , is now defined on page 1338 line 7

36  
37 **15. equations 8 and 9. Provide a reference for this definition of a centroid. Doesn’t it have a  
38 fundamental problem when polygons intersect, such as we see in Fig. 2 at a scale of 5 years  
39 around 1990?**

40  
41 A reference (Worboys and Duckham, 2004) has been added on page 1338 line 12. Although  
42 graphically the polygons appear to be intersecting, problems in computing the centroids have never  
43 arose because the polygons don’t actually intersect when examined more closely.

44  
45 **16. pg 1340 line 3. Why is it “...noted that all holes...” When would holes be relevant for this  
46 procedure? Please clarify or remove.**

1  
2 The exclusion of holes in the calculation of holes is now justified on page 1340 line 3. The convex  
3 hull is not defined for sets with holes because line segments can always leave sets containing holes.

4  
5 **17. pg 1340 line 14. Do patches of equal area “need to be distinguished”? I would think that**  
6 **they should have the same significance that would depend on how often they occur.**

7  
8 The procedure has been changed to not include convexity in the calculation of the null distribution,  
9 though the removal of convexity was found to make the test, on average, less conservative than  
10 the areawise test. Instead, convexity is now used to explain differences between the areawise and  
11 geometric tests in Sect. 4.2.

12  
13 **18. pg 1340 line 17. I don’t understand why two patches with the same normalized significant**  
14 **area, regardless of shape, don’t have the same significance. The authors need to better**  
15 **motivate in what context this difference in geometry matters. One could simply be testing**  
16 **the area without regard to this shape issue. If there was no reliance on the reproducing kernel**  
17 **(which becomes less and less relevant for strongly auto- correlated noise), the test should be**  
18 **on the distributions of A and nothing else.**

19  
20 After a careful investigation, it was determined that convexity only plays a minor role in the testing  
21 procedure but still remains an essential part of the manuscript. See responses to comments 17 and  
22 21.

23  
24 **19. pg 1340 line 20. Is the null distribution of chi independent of the form of the null**  
25 **hypothesis noise? If not, then the dependence should be explicitly stated here.**

26  
27 The choice of null hypothesis does not seem to impact the null distribution substantially. The lack  
28 of dependence on the lag-1 autocorrelation coefficients is now explicitly stated on page 1340 line  
29 20.

30  
31 **20. pg 1343 line 2. The “large number” should be stated. Their length in time should also be**  
32 **stated. Does the length matter?**

33  
34 “Large number” has been change to “1000” on page 1343 line 2. The length of the time series were  
35 1000. The length of the time series does matter, at least for the pointwise significance levels used  
36 in this study.

37  
38 **21. pg 1343 line 10. How should one interpret the differences between the two tests? If a patch**  
39 **is areawise significant but not geometrically significant in particular, seems to possibly point**  
40 **to a substantial issue in the testing procedures, a problem with including convexity in the**  
41 **geometric procedure, or a problem with the reproducing kernel approach in both tests.**  
42 **These discrepancies need to be addressed and discussed in depth, as it goes to the heart of**  
43 **the point of this paper.**

44  
45 The differences between the two tests arise from the fact that implicit in the calculation of areawise  
46 significance level are the convexity and other geometric parameters of a typical patch generated

1 from red noise. An in-depth discussion has been added on page 1343 line 10 describing the  
2 difference between the two tests and how such differences should be interpreted.  
3 Two additional paragraphs have been added:  
4 “According to the areawise test, patches with smaller values of  $\mathcal{C}$  are less likely to be areawise  
5 significant so that it is expected that patches deemed significant by the areawise test will be  
6 primarily convex. To test this hypothesis, 10,000 patches arising from red-noise processes with  
7 different lag-1 autocorrelation coefficients were generated and the convexity of those patches  
8 deemed areawise significant at the  $\alpha_{aw} = 0.05$  level was calculated. The results in Fig. 6c show  
9 the mean convexity as a function of the lag-1 autocorrelation coefficients, together with the 95%  
10 confidence bound. The mean convexity of the patches was found to be approximately 0.8,  
11 regardless of the lag-1 autocorrelation coefficient. An identical experiment was also performed for  
12 geometrically significant patches but with the convexity of patches that are geometrically  
13 significant at the  $\alpha_{geo} = 0.05$  being computed. In contrast to areawise significant patches, patches  
14 that were found to be geometrically significant, on average, had lower convexity, the reason for  
15 which is that the calculation of  $\alpha_{geo}$  makes no assumption about convexity. The  $p$ -value for the  
16 geometric test is thus  $p_{geo} = f(A; H_0)$  for some function  $f$ , contrasting with  $p_{aw}$  that depends on  
17 convexity. The results of the experiments are consistent with Figs. 5a and 5b, where both the ideal  
18 patches have the same geometric significance but the ideal patch in Fig. 5b has a larger  $p_{aw}$  so that  
19  $p_{aw} > p_{geo}$ .”  
20 “Convexity cannot fully explain the differences between  $p_{aw}$  and  $p_{geo}$  for a given patch. More  
21 generally,  $p_{aw} = g(\mathcal{C}, A, S_1, \dots, S_R; H_0)$ , where  $S_1$  to  $S_R$  are shape parameters of the patch, such as  
22 aspect ratio and symmetry. For example, for a convex patch whose length in the time direction is  
23 long with respect to the reproducing kernel (at some critical level) but thin in the scale direction  
24 with respect to the reproducing kernel would be deemed insignificant by the areawise test, though  
25 it may have an area much larger than the critical area of the areawise test. Asymmetry with respect  
26 to the scale axis, as another example, may also result in a patch being deemed insignificant by the  
27 areawise test if, for example, the width of the patch in the scale direction decreases with time. If  
28 the normalized areas of such patches are larger than the critical level of the geometric test, the  
29 patches will be geometrically significant, though may not be areawise significant if the  
30 reproducing kernel is unable to fit inside the narrow portion of the patch. The above arguments  
31 suggest that  $f(A; H_0) \neq g(\mathcal{C}, A, S_1, \dots, S_R; H_0)$  and thus the significance of patches as determined  
32 by the geometric and areawise tests need not be equal.”

33  
34 **22. pg 1343 line 17. Why is significance level of 0.9 being used (I think you mean 0.1). Why**  
35 **not 0.05, as it more common and reduces the risk of the Type I error more?**

36  
37 The significance level has been changed to 0.05 for the areawise test to reduce Type 1 errors.

38  
39 **23. pg 1343 lines 25-27. The multiple testing problem is still not resolved, at least in this**  
40 **discussion and application of the test. In Fig. 1, I see more than 20 patches and 3 are**

1 **geometrically significant. Couldn't I have gotten that result from chance at the 10% level of**  
2 **the test?**

3

4 The authors appreciate the critical evaluation of the proposed method. The motivation for  
5 constructing the geometric test was to offer an alternative method for dramatically reducing the  
6 number of spurious results. However, a simple way of further reducing spurious results detected  
7 using the geometric test is to apply the Benjamini and Hochberg (1995) method to the  $p$ -values of  
8 individual patches in a given wavelet power spectrum to control the false discovery rate, the  
9 expected proportion of rejected null hypotheses that are actually true. A discussion of the method  
10 has been added to page 1342 and the method has been used throughout the text.

11 Section 4.2 includes the following discussion of the Benjamini and Hochberg (1995) procedure:

12 “If the geometric test was performed on  $K$  significance patches at the  $\alpha_{geo}$  level, then, on average,  
13 one can expect  $\alpha_{geo}K$  false positive results, which would make the geometric test permissive for  
14 large  $K$ . It is therefore necessary to reduce the number of false positive results. There are various  
15 ways to reduce the number of false positives, including the Walker test, Bonferroni correction, and  
16 other counting procedures (Wilks, 2006). Recently, methods for controlling the false discovery  
17 rate (FDR) have been developed, where the FDR is the expected proportion of rejected local null  
18 hypotheses that are actually true (Benjamini and Hochberg, 1995). In particular, Benjamini and  
19 Hochberg (1995) developed a method for controlling the FDR based on the number of local  
20 hypotheses being tested and the degree to which the local hypotheses were rejected, contrasting  
21 with other procedures that ignore the confidence with which the local tests reject the local  
22 hypotheses (Wilks, 2006). Moreover, the method has proven to have high statistical power,  
23 especially when only a small fraction of the  $K$  local tests correspond to false null hypotheses  
24 (Wilks, 2006). The procedure will therefore be used to control the false discovery rate of the  
25 geometric test, which will facilitate the interpretation of results.

26 Suppose that  $K$  local hypotheses were tested, where, in present case, the local hypotheses refer to  
27 the testing of each patch individually under the assumption that the results of the individual tests  
28 are independent. A global geometric test can be performed at the  $\alpha_{global}$  level as follows: Let  $p_{(l)}$   
29 denote the  $l$ th smallest of  $K$  local  $p$ -values; then, under the assumption that the  $K$  local tests are  
30 independent, the FDR can be controlled at the  $q$ -level by rejecting those local tests for which  $p_{(l)}$   
31 is no greater than

32 
$$p_{FDR} = \max_{r=1, \dots, K} [p_{(r)} : p_{(r)} \leq q(r/K)] \quad (15)$$

33 
$$\max_{r=1, \dots, K} [p_{(r)} : p_{(r)} \leq \alpha_{global}(r/K)] \quad (16)$$

34 so that the FDR level is equivalent to the global test level. According to the procedure, any local  
35 test resulting in a  $p$ -value less than or equal to the largest  $p$ -value for which Eq. (16) is satisfied is  
36 deemed significant. If no such local  $p$ -values exist, then none are deemed significant and, therefore,  
37 the global test hypothesis cannot be rejected. The global geometric test will thus only deem those  
38 significant patches with  $p$ -values satisfying Eq. (16) as significant. Throughout the paper  
39  $q = \alpha_{global}$  will be set to 0.05.”



1  
2 **24. pg 1343 line 27. I don't see any obvious seasonality in the wavelet power spectrum shown.**  
3 **The time-averages of the wavelet power for each season would help to make the "variability"**  
4 **point. It is currently not supported by the figure.**

5  
6 Line 27 on page 1343 was removed because the modified geometric test did not find any significant  
7 patches.

8  
9 **25. pg 1344 line 3 and following. I don't see a period of 32 months or of 12 months plotted on**  
10 **the figure 2. It only goes to a period of 7 months.**

11  
12 The axis label is incorrect and should be "years." However, to be consistent with other plots the  
13 axis labels and limits have been set to months in Figure 2.

14  
15 **26. pg 1344 line 26. The definition and method of calculating a "hole" needs to be given.**

16  
17 A formal a definition of a "hole" has been inserted on page 1344 line 26. The definition uses  
18 notions from topology to define what it means for a patch to contain a hole.

19  
20 **27. pg 1345 line 1. What is the sensitivity of the shape and amplitude of Fig. 5 to the choice**  
21 **of autocorrelation. Would 0.9 and 0.1 be different or the same? The authors are making**  
22 **generalizations based on just one parameter setting.**

23  
24 The amplitude of Fig. 5 was found to be independent of the autocorrelation coefficient. Such a  
25 lack of dependence has been explicitly stated on page 1345 line 1.

26  
27 **28. pg 1345 line 11. Why is an 80% significance level used here? 90% was used earlier. Both**  
28 **have a larger risk of a Type I error than the traditional 95%. (note that the nomenclature**  
29 **should actually be 20%, 10%, and 5% when the "significance" is being considered rather**  
30 **than the error bar).**

31  
32 In this case, a pointwise significance level of 20% is used to find "holes" and not to assess the  
33 significance of the wavelet coefficients squared. The nomenclature on page 1345 line 11 has been  
34 changed to 20%, 10%, and 5%. The nomenclature in all the figures and figure captions have been  
35 changed as well.

36  
37 **29. pg 1345 and following. What null hypothesis is being compared in this simple test of white**  
38 **noise and a sinusoid. How different were the amplitudes? Is this actually a general result or**  
39 **specific to the parameters chosen for the series? A similar lack of specificity and detail**  
40 **applies to the rest of the discussion through page 1349. The**  
41 **results only have theoretical implications if they are generalizable. From the present**  
42 **discussion, this cannot be assessed.**

43  
44 The authors appreciate the reviewer's careful reading of pages 1345-1349 and constructive  
45 criticism. The comments have resulted in significant improvements to this part of the manuscript.

1 The null hypotheses used were white noise and red-noise spectra. Their uses are now explicitly  
2 stated on page 1345 lines 16 and 17. For the experiment of a single sine wave, sine waves of  
3 varying amplitudes were generated to determine if there is an amplitude dependency. It was  
4 determined that there was no amplitude dependence, which is now explicitly stated on page 1345  
5 line 16.

6 A discussion of several other experiments has been added to Section 5.1 page 1348 in order to test  
7 how the results would change under a different set of parameters. The additional experiments  
8 include using different noise backgrounds, amplitude of the cosines, and signal-to-noise ratios. It  
9 turns out, however, that there is only a small difference between the theoretical critical delta  $r$  for  
10 the original experiment and that obtained under very low-noise situations with the cosines having  
11 large amplitudes. The low-noise, high-amplitude situation is considered the best-case scenario so  
12 that it represents a theoretical maximum.

13  
14 The following paragraph has been added to address the reviewer's concerns:

15 "It turns out that even if the above experiment (not shown) was repeated using white-noise  
16 background spectra  $\Delta r_{crit}$  would still be equal to 0.45, though more holes were found to appear at  
17 signal-to-noise ratios less than 2. It was expected, however, that  $\Delta r_{crit}$  also depends on the  
18 amplitudes of the cosines in Eq. 24. Thus, a third experiment was conducted in which the  
19 amplitudes of the cosines were allowed to vary from 1 to 50 and  $f_1$  and  $f_2$  were allowed to vary  
20 from 0 to 0.5. The experiment was repeated for signal-to-noise ratios from 1 to 20. The results  
21 from the experiments (not shown) indicate that for red-noise background spectra and for a signal-  
22 to-noise ratio of 20 that  $\Delta r_{crit} = 0.53$ , contrasting with the case for white noise background spectra  
23 where  $\Delta r_{crit}$  was found to be 0.51."

24 Overall, the discussions from pages 1345 through 1349 have been refined by including more  
25 details of the experiments performed.

26  
27 **30. pg 1349 line 9. Couldn't the same effect be found in the linear AR2 model for some choices**  
28 **of its two parameters? I don't think that nonlinearity needs to be invoked to see this behavior**  
29 **of "holes".**

30  
31 An AR2 process could certainly produce holes but not to the extent that a nonlinear time series  
32 could. In fact, the amount of holes generated from AR2 processes was found to be similar to that  
33 of AR1 processes.

34  
35 **31. pg 1349 line 19. What is meant by "phase coherent oscillations"?**

36  
37 A definition of phase coherence was added to page 1349 line 19.

38  
39 **32. Is there a sensitivity to the  $dj$  used in the wavelet analysis? If so, this should be stated.**

40  
41  $dj$  controls the spacing between discrete scales, where a smaller  $dj$  will give better scale resolution.  
42 If the  $dj$  is too large there will not be adequate sampling in scale so that some features will be  
43 missed. The maximum value of  $dj$  depends on the analyzing wavelet used, though  $dj$  is not intrinsic  
44 to the wavelet function so sensitivity of results to  $dj$  seems unlikely.

45

1 **If  $d_j$  is somehow intrinsic to the wavelet function, this should be referenced or shown. I do**  
2 **not know of any support for this idea. It is a tunable parameter as far as I know.**

3  
4 To the authors knowledge,  $d_j$  is not intrinsic to the wavelet function itself but to how the scales are  
5 discretized.

6  
7 **33. Fig. 1. I recommend some other symbol or method to indicate the geometrically**  
8 **significant patches. Stippling or hatching them would help them better stand out. The  $x$**   
9 **makes me think that these patches have been eliminated, rather than highlighted.**

10  
11 Gray shading has been used to highlight those significance patches that are geometrically  
12 significant and thick red contours are used to indicate the areawise significance regions in Figs. 1  
13 and 2 (now Figs. 3 and 4).

14  
15 **34. Fig. 1. The “ $I_{sim}$ ” indicated on the figure should be defined in the caption.**

16  
17 Because the false discovery rate is used in the ideal and climatic examples,  $I_{sim}$  no longer appears  
18 on Figs. 1 and 2 now (Figs. 3 and 4) and related figures.

19  
20 **35. Fig. 1, Somewhere the actual wavelet spectral values should be shown to get a sense of**  
21 **how the regions passing the pointwise test compare to those not passing.**

22  
23 For clarity, the full wavelet power spectra have been plotted separately from the areawise and  
24 geometric test results and are now Figs. 1 and 2. The results for the areawise and geometric tests  
25 are now Figs. 3 and 4.

26  
27 **36. Fig. 1. I don't see in the text where “normalized” has been defined.**

28  
29 Normalized wavelet power has now been defined on page 1335 line 16.

30  
31 **37. The red noise equation being used should be shown and how the parameters are fit should**  
32 **be stated. Some discussion of why one is testing against discrete red noise compared to**  
33 **continuous red noise should be given. The spectra are not the same.**

34  
35 The red-noise equation used is now shown on page 1335 line 12 and the equation for a theoretical  
36 red-noise background is also shown. Two methods are now cited that are used for estimating AR1  
37 parameters in Sect. 3.1. A discussion of those methods seems beyond the scope of the paper so  
38 that the reader is referred to books describing them in-depth. The use of a discrete red-noise  
39 spectrum was discussed in Torrence and Compo (1998) and has since been routinely applied to  
40 wavelet power spectra of climatic time series. Instead of adding a discussion of the use of a discrete  
41 Fourier spectrum in wavelet analysis, which would add to the overall length of the paper, the reader  
42 is referred to Torrence and Compo (1998) for a more in-depth discussion.

43  
44 **38. Why are Fig. 1 and Fig 2 plotted so differently? Also, please double check that the time**  
45 **series in Fig 2a is monthly resolution. It does not appear to be monthly. It looks like it has**  
46 **been smoothed.**

1  
2 Figs. 1 and 2 are now plotted identically. See response to comment 12. The data were checked and  
3 found to be monthly resolution.

4  
5 **39. Why are such short time series considered? The NAO extends back to the early 1800s.**  
6 **Nino3.4 goes back to 1850 in several datasets. I would think that the longest possible record**  
7 **would help in defining the distribution of areas. It would also push out the cone of influence.**

8  
9 Longer time series for the NAO and Nino 3.4 index are used throughout the paper. In particular,  
10 the time period has been extended to 1870-2013 to better illustrate the applicability of the proposed  
11 methods.

12  
13 **40. pg 1350 line 10. No one has shown that “spurious results” are “ubiquitous” in wavelet**  
14 **spectra and neither has this paper. In contrast, Maraun et al. 2007 showed (Appendix C)**  
15 **that the sensitivity of pointwise and areawise tests depends on the signal to noise of the series.**  
16 **As exemplified in the discussion of Fig. 1, this geometric test still has the multiple testing**  
17 **problem.**

18  
19 We agree. Line 10 on page 1350 has been deleted.

## 20 21 **Technical corrections**

22  
23 **1. pg 1338 “would have it did not contain” needs an “if”. 2. Fig. 2. I think something is wrong**  
24 **with the y-axis as given. Nino3.4 should not have so much power at periods of 5 months and**  
25 **the cone-of-influence for monthly data should be at much longer scales than 7 months**

26  
27 The text on page 1338 has been corrected. The labels on the y-axis should have been months, not  
28 years. The axis label and axis limit of Fig. 2 have been corrected.

## 29 30 **Reviewer 2**

31  
32 **The manuscript describes new methodology for advancing statistical significance testing of**  
33 **wavelet power spectra. The methodology builds from previous work in significance testing**  
34 **and addresses several problems that previous work did not address. The manuscript is**  
35 **generally very well written and concise, in particular given that it blends sophisticated time-**  
36 **frequency decomposition, statistical, and topological concepts. The work represents**  
37 **advancement in the quantitative interpretation of wavelet analysis, which is a topic that has**  
38 **received criticism. Therefore, I recommend it for publication in Nonlinear Processes in**  
39 **Geophysics. However, I have several general and specific comments that should be addressed**  
40 **before publication.**

41  
42 We are grateful for these thoughtful comments, which are addressed in detail in the responses to  
43 the general and specific comments listed below.

1 **General comments**

2  
3 **(1) The manuscript describes significance testing based on geometric and topological**  
4 **properties of regions within the wavelet power spectrum. These properties are closely tied to**  
5 **the parameters of the wavelet. The manuscript only considers the Morlet wavelet with  $\omega_0=6$ .**  
6 **The authors should discuss the sensitivity of their results to other commonly used wavelets**  
7 **or wavelet parameters that provide more (less) precision in the time domain and less (more)**  
8 **in the frequency domain compared to Morlet.**

9  
10 The reviewer is correct that the results are sensitive to the analyzing wavelet, but we believe that  
11 a complete exposition of this point is beyond the scope of this paper because the Morlet wavelet  
12 is suitable for most geophysical applications; discussion of other wavelets in this context is mainly  
13 of mathematical interest. The following brief discussion of the sensitivity of the results to the  
14 chosen analyzing wavelet has been included in the summary section (Sect. 7):

15 “It is noted that the geometric test was only applied to patches arising from the convolution of the  
16 Morlet wavelet with a time series. The results presented in this paper are not valid for wavelet  
17 power spectra obtained using other analyzing wavelets, the reason for which is that each wavelet  
18 function has different time- and scale-localization properties that inevitably impact the geometry  
19 of patches. For example, patches found in the wavelet power spectrum obtained using a Paul  
20 wavelet are elongated in the scale direction relative to those obtained using a Morlet wavelet with  
21  $\omega_0 = 6$ , resulting in nearby patches at different scales merging together. The merging of patches  
22 at different scales will alter their geometry with respect to the relatively thin (in scale) patches  
23 obtained using the Morlet wavelet.”

24  
25 **(2) What is the purpose of using the NAO time series as an example to assist with describing**  
26 **and testing the new methods? After it is introduced, it is largely dismissed as being a poor**  
27 **choice for this task and the focus shifts to the Nino 3.4 index.**

28  
29 The idea behind using the NAO index was to show, using the new methods, that the NAO is a  
30 stochastic process. Climate implications have been added to the paper to better motivate the use of  
31 the NAO in the application of the methods. Feldstein (2002), for example, found the NAO to be  
32 consistent with a first-order Markov process with a typical lifetime of 7 to 10 days. Hanna et al.  
33 (2014), as an another example, found that the variability of the NAO has increased but the results  
34 from geometric test suggests that such changers have been stochastic in nature.

35  
36 **(3) The Cone of Influence (COI) is referenced in the figure captions, but not described in the**  
37 **text. For pointwise significance, identifications are independent, so pointwise significance**  
38 **outside the COI can be ignored in the same way that wavelet power can be ignored outside**  
39 **the COI. It seems like this might not be true for geometric and topological methods.**  
40 **Therefore, are topological and geometric tests sensitive to edge effects (i.e., can edge effects**  
41 **influence significance even in regions where power is not influenced by edge effects)? If so,**  
42 **please provide more information about the importance of the COI and how it might influence**  
43 **results using the proposed methods.**

1 The definition of the COI has been added on Page 1335 line 16. The cone of influence is the region  
2 of the wavelet spectrum in which edge effects become important. The areawise, geometric, and  
3 topological methods are all sensitive to edge effects. The effect of the COI on a patch located  
4 outside the COI is to shrink the patch, as the wavelet power and thus the significance associated  
5 with the patch are reduced. A paragraph discussing the impact of the COI on the results of the  
6 geometric test has been added after line 10 Page 1342. The paragraph reads as follows:

7 “Another situation that may arise in practice is the application of the geometric test to patches  
8 located both inside and outside the COI. In the case of the pointwise significance test, the edge  
9 effects only influence those wavelet power coefficients that lie inside the COI; however, for the  
10 geometric test, the significance of the entire patch will be impacted even if the patch only partially  
11 lies inside the COI. The reason is that the COI will act to decrease the size of significance patches  
12 through the reduction of wavelet power in the COI and subsequently the total area of the patch.  
13 One should thus be cautious when interpreting the results of the geometric test for patches near the  
14 COI.”

15  
16 **(4) Significance is determined by the 90% confidence level for the areawise and geometric  
17 tests, but 95% is used for the pointwise test. What is the reason for this inconsistency?**

18  
19 Throughout the paper we now use the 95% confidence level for the pointwise and areawise tests.  
20 The false discovery rate of the geometric test is controlled at the 5% level

21  
22 **(5) Throughout the text and captions, Figures 1, 2, 6, and 7 are described as “wavelet power  
23 spectra”, but wavelet power is not shown in the figures. The authors should find another way  
24 to describe the contents of the figures or include contours of wavelet power.**

25  
26 “Wavelet Power Spectra” are now referred to as the significance of wavelet power  
27 throughout figure captions and text.

28  
29 **(6) There is no discussion about how “holes” are identified and I don’t feel that there is  
30 enough information for future work to adopt the method. Minimally, holes should be defined  
31 quantitatively somehow, but it might also be helpful to describe how an algorithm could be  
32 developed to identify them. I am further confused because I cannot see all the holes that are  
33 identified in Figure 6 and 7, in part perhaps because the wavelet power is not shown, and in  
34 part because the significance patch does not completely encircle them.**

35  
36 A formal definition of a hole has been added on page 1344 line 19. Moreover, a discussion of how  
37 a hole is calculated is also provided after the definition is given. The following text has been added  
38 to include the definition of a hole:

39 “A more formal definition of a hole will require some notions from topology. Let  $I = [0,1]$  be the  
40 close unit interval. Then a path from a point  $a$  to a point  $b$  in a significance patch  $P$  is a continuous  
41 function  $f: I \rightarrow P$  with  $f(0) = a$  and  $f(1) = b$ , where in the case that  $f(0) = f(1) = c$  the path is said  
42 to be closed (Hatcher, 2002). Note that a point is a special kind of closed path called the constant  
43 path. A patch will be said to contain a hole if there exists a path in the significance patch such that  
44 it cannot be continuously deformed into a point, where the feature obstructing the path from such

1 a deformation is a hole. The definition is consistent with notions of simply-connectedness in  
2 topology (Hatcher, 2002). Figure 4 shows an example of a closed path (blue curve) in a patch that  
3 cannot be contracted to a point because it surrounds a hole located in the patch.”  
4

5 The calculation of a hole is discussed in the following paragraph:

6 “For a patch with a hole, there will be two boundaries, an external boundary and an internal  
7 boundary representing the boundary between the hole and the patch. Thus, if a patch contains an  
8 internal boundary or contour it will contain a hole, whereas a patch without a hole will contain no  
9 internal contours. In practical applications, the existence of a hole can be determined by orienting  
10 external contours in the clockwise direction and internal contours in the counter-clockwise  
11 direction, a procedure automatically implemented using the standard Matlab contour function. The  
12 number of counter-clockwise oriented contours is thus the number of holes in the wavelet power  
13 spectrum at a given pointwise significance level.”

14 Figures 6 and 7 have been changed so that the reader can identify the location of the holes at  
15 different pointwise significance levels. Table 1 has also been changed to better illustrate the power  
16 of the topological method in identifying significant wavelet power coefficients. The discussion in  
17 Sect. 5 has been changed to reflect the changes in Table 1 and Figs. 6 and 7 (now Figs. 8 and 9).

## 18 19 **Specific Comments**

20  
21 **(1) S1333L20: To better orient the reader, can you please provide a sentence or two that**  
22 **describes the main problems with pointwise testing?**

23  
24 Added on page 1333 line 21 is a brief example of what would happen if the pointwise significance  
25 test was applied to a wavelet power spectrum with a large number of wavelet power coefficients.  
26 The example will better orient the reader.

27 **(2) S1335L16-18: This sentence should reference Figure 1.**

28  
29 Figure 1 has been referenced on page 1335 line 16.

30  
31 **(3) S1335L18-20: This sentence should reference Figure 2. The sentence states that periods**  
32 **from 16 to 64 months are significant, but Figure 2b only goes from 1 to 7 months. I suspect**  
33 **that the axis is actually in years or that the values are  $j$  not  $s_j$ . However this is resolved it**  
34 **would be good to maintain consistency between Figs. 1 and 2.**

35  
36 Figure 2 has been referenced on page 1335 line 18. The scale axis has been corrected (should be  
37 months and labeled in months).

38  
39 **(4) Section 3.1: Please define the term “patch”. Section 3.1 is good place to define the term**  
40 **similarly to how it is defined in the captions to Figs. 1 and 2, but the introduction might be a**  
41 **good place too.**

42  
43 The definition of a patch was added to page 1333 line 23.

1  
2 **(5) S1336L5: Can this sentence be rearranged to define a and b at the beginning? Also, is it**  
3 **necessary to use b and a? Does  $b = t$  appendix A and does  $a = s$  appendix A ?**

4  
5 The notation has been changed from  $b$  to  $t$  and from  $a$  to  $s$  throughout Sect. 2 and in Appendix A.

6  
7 **(6) S1336L15-17: This sentence is not quite clear. If a kernel fits within the patch is the entire**  
8 **continuous patch interpreted as significant or only the points that fall within the kernel?**

9  
10 Two sentences have been added on page 1336 line 16 to clarify that only points within the kernel  
11 should be deemed significant.

12  
13 **(7) Section 4.1: It would be helpful to lead this section (or alternatively close the previous**  
14 **section) with a sentence that reminds the reader of the objectives of the developing a new**  
15 **geometric test to improve upon the areawise test.**

16  
17 A short paragraph has been inserted in the beginning of Sect. 4.1 to explicitly state the objectives  
18 of the test and to motivate the reader before the geometric test is developed. The paragraph reads  
19 as follows:

20 “A disadvantage of the areawise test is the complexity of the  $\alpha_{aw}$  calculation, which involves a  
21 root-finding algorithm. It is therefore desirable to construct an alternative test whose significance  
22 level is easy to calculate, readily allowing the following: (1) the application of the test to patches  
23 at various pointwise significance levels; (2) the adjustments of the significance level of the test;  
24 (3) the application of the test to wavelet power spectra obtained using other analyzing wavelets;  
25 and (4) the implementation of  $p$ -value adjustment procedures to control the family-wise error rates  
26 and false discovery rates.”

27  
28 **(8) S1337L15 & Eq. 6: Please define  $j$ . Shouldn't it be  $t_n$  and  $s_j$  instead of  $t_i$  and  $s_i$  since  $s$  and**  
29  **$t$  are independent ( $n$  need not equal  $j$ ) and also have different maximum values (i.e.,  $J \neq N$ )?**  
30 **Thus,  $p_{n,j}$  not  $p_i$ ?**

31  
32  $s_j$  has been defined on page 1337 line 15. The  $j$  now refers to the  $j$ th scale value in the set of scales  
33 determined by the equation inserted after Eq. (6). Notation has been changed to ensure consistency  
34 among the different indices such as  $i$  and  $j$ .

35  
36 **(9) S1338 Equations: Again, I'm confused about  $i$ . I think it is used appropriately for  $t$ , but**  
37 **the index of  $s$  is an entirely different coordinate than that of  $t$ . additionally,  $n$  is defined as**  
38 **the index of time (1 to  $N$ ) in Eq. (2). It seems to be redefined here.**

39  
40 Yes, the indices are not used appropriately for  $s$ . To remedy the problem, notation has been  
41 changed throughout Sect. 4 so that the indices are consistent. Instead of redefining  $n$ ,  $m$  has been  
42 used to denote the number of vertices of the polygon for Eqs. (7), (8), and (9) (now Eqs. (11), (12),  
43 and (13)).

44  
45 **(10) S1340L24: The  $p$ -value here is not the same as  $p$  in S1337L15, yes?**



1  
2 The  $p$  on page 1337 line 15 is not same as the  $p$ -value on page 1340 line 24. A change of notation  
3 has been made to reflect that on page 1337 line 15.

4  
5 **(11) S1346L18: Is “top panel” actually the bottom panel (Fig. 6c)?**

6  
7 “Top Panel” has been changed to “Fig. 6c” on page 146 line 18.

8  
9 **(12) Captions for Figures 1 and 2: It might be helpful to call out relevant sections throughout**  
10 **the captions, as was done for Fig. 2a.**

11  
12 The reader is now referred to specific sections in the text in the captions for Figs. 1 and 2 (now  
13 Figs. 3 and 4).

14  
15 **(13) Caption for Figure 3: Please clarify in the caption that the reproducing kernel is**  
16 **associated with the areawise test and not the geometric test, but is shown for reference.**

17  
18 A clarification sentence has been added in the caption of Fig. 3 (now Fig. 5), indicating that the  
19 reproducing kernel is for the areawise test.

20 **References added**

21 Baxandall, P. and Liebeck, H.: Vector Calculus, Dover Publications, INC., Mineloa, New York,  
22 550, 2008. Benjamini, Y. and Hochberg, Y.: Controlling the False Discovery Rate: A Practical  
23 and Power Approach to Multiple Testing, J. Roy. Stat. Soc., 57, 289-300, 1995.

24 Benjamini, Y. and Hochberg, Y.: Controlling the False Discovery Rate: A Practical and Power  
25 Approach to Multiple Testing, J. Roy. Stat. Soc., 57, 289-300, 1995.

26 Benjamini, Y. and Yekutieli, D.: The Control of the False Discovery Rate in Multiple Testing  
27 under Dependency, Ann. Stat., 29, 1165–1188, 2001.

28 Feldstein, S. B.: The Time Scale, Power Spectra, and Climate Noise Properties of Teleconnection  
29 Patterns, J. Climatol., 13, 4430-4440, 2000.

30 Hasselmann, K.: Stochastic Climate Models Part I. Theory, Tellus. , 28, 473-485, 1976.

31 Hatcher, A.: Algebraic Topology, Cambridge University Press, New York, 544, 2001.

32 Hanna, E., Cropper, T. E., Jones, P. D., Scaife, A. A., and Allan, R.: Recent seasonal asymmetric  
33 changes in the NAO (a marked summer decline and increased winter variability) and associated  
34 changes in the AO and Greenland Blocking Index, Int. J. Climatol., 2014.

35 Kay, S. M.: Modern Spectral Estimation: Theory and Application, Prentice Hall, Englewood  
36 Cliffs, NJ, 560, 1988.

1 Wilks, D. S.: On “Field Significance” and the False Discovery Rate, *J. Appl. Meteor. Climatol.*,  
2 45, 1181-1189, 2006.

3 Worsby, F. M., Duckham, M.: *GIS: A Computing Perspective*, CRC Press, Boca Raton, FL, 448,  
4 2004.

5

6

# 1 Geometric and topological approaches to significance testing in wavelet analysis

2 J. A. Schulte<sup>1</sup>, C. Duffy<sup>2</sup>, and R.-G. Najjar<sup>1</sup>

3 [1] Department of Meteorology, The Pennsylvania State University, University Park,  
4 Pennsylvania

5 [2] Department of Civil Engineering, The Pennsylvania State University, University Park,  
6 Pennsylvania

7 Correspondence to: J. A. Schulte (jas6367@psu.edu)

8

9

## Abstract

10 Geometric and topological methods are applied to significance testing in the wavelet domain. A  
11 geometric test was developed for assigning significance to pointwise significance patches in local  
12 wavelet spectra, contiguous regions of significant wavelet power coefficients with respect to some  
13 noise model. This geometric significance test was found to produce results similar to an existing  
14 areawise significance test while being more computationally flexible and efficient. The geometric  
15 significance test can be readily applied to pointwise significance patches at various pointwise  
16 significance levels in wavelet power and coherence spectra. The geometric test determined that  
17 features in wavelet power of the North Atlantic Oscillation (NAO) are indistinguishable from a  
18 red-noise background, suggesting that the NAO is a stochastic, unpredictable process, which could  
19 render difficult the future projections of the NAO under a changing global system. The geometric  
20 test did, however, identify features in the wavelet power spectrum of an El Niño index (Niño 3.4)  
21 as distinguishable from a red-noise background. A topological analysis of pointwise significance  
22 patches determined that holes, deficits in pointwise significance embedded in significance patches,  
23 are capable of identifying important structures, some of which are undetected by the geometric  
24 and areawise tests. The application of the topological methods to ideal time series and to the time  
25 series of the Niño 3.4 and NAO indices showed that the areawise and geometric tests perform  
26 similarly in ideal and geophysical settings, while the topological methods showed that the Niño  
27 3.4 time series contains numerous phase-coherent oscillations that could be interacting nonlinearly.

28

## 1. Introduction

29 Time series are often complex, composed of oscillations and trends. The goal of researchers is  
30 to decide whether the embedded structures in the time series are stochastic or deterministic. Such  
31 decisions can be made using Fourier analysis, with the assumption that the underlying time series  
32 is stationary (Jenkins and Watts, 1968). In many cases, however, the stationary assumption is not  
33 satisfied, making Fourier analysis an inappropriate tool for feature extraction. For non-stationary  
34 time series, wavelet analysis (Meyers, 1993; Torrence and Compo, 1998) can be used for

1 decomposing a time series into both frequency and time components, allowing the extraction of  
2 transient features and dominant modes of variability. Once embedded structures in time series have  
3 been identified, a natural question arises: what physical mechanisms are responsible for the  
4 detected modes of variability? Linkages between the modes of variability and possible physical  
5 mechanisms can be obtained using wavelet coherence (Grinsted et al., 2004), a bivariate tool for  
6 detecting common oscillations between two time series. Together, wavelet power and coherence  
7 analyses have proven useful in climate science (Velasco and Mendoza, 2007; Muller et al., 2008),  
8 hydrology (Zhang et al., 2006; Ozger et al., 2009; Labat, 2008; Labat, 2010), atmospheric science  
9 (Terradellas et al., 2005; Schimanke et al., 2011), and oceanography (Lee and Lwiza, 2008).

10 The application of wavelet analysis alone is not sufficient for feature extraction of time series;  
11 indeed, random fluctuations can produce large values of spectral power or coherence related to the  
12 underlying process (e.g., red-noise) and not necessarily the time series. In Fourier analysis, one  
13 chooses a suitable noise model and assesses the significance of features relative to some  
14 analytically or empirically derived threshold. In climate science, for example, one often compares  
15 the sample power spectrum of a time series to that of a theoretical red-noise [spectrum \(Hasselmann,  
16 1976; Torrence and Compo, 1998\)](#). Statistical significance testing is also necessary in the wavelet  
17 domain. Torrence and Compo (1998) were the first to assess the significance of features in wavelet  
18 power spectra using discrete red-noise background spectra. Grinsted et al. (2004), using Monte  
19 Carlo methods, extended significance testing to wavelet coherence using surrogate red-noise time  
20 series. The (pointwise) significance tests developed by Torrence and Compo (2010) and Grinsted  
21 et al. (2004), however, have multiple-testing problems, given the large number of wavelet  
22 coefficients being tested simultaneously (Maraun and Kurths, 2004). [Suppose, for example, that a  
23 pointwise significance test was applied to  \$M\$  wavelet power coefficients at the 5% significance  
24 level. Then, on average, there will be  \$0.05M\$  false positive results, which would make the pointwise  
25 test permissive for large  \$M\$ . Maraun et al. \(2007\) addressed these problems by developing an  
26 areawise test that sorts through contiguous regions of pointwise significance called significance  
27 patches based on their area and geometry, minimizing spurious results, and thus giving researchers  
28 more insight into the time series in question. According to the areawise test, the larger the  
29 pointwise significance patch, the less likely it was generated from a stochastic fluctuation.](#)

30 In this study, significance testing in the wavelet domain is improved through the following: (1)  
31 the development of a flexible and computationally efficient geometric test capable of minimizing  
32 spurious results from the pointwise test by associating  $p$ -values to individual patches in wavelet-  
33 power and wavelet-coherence spectra; and (2) the application of topological methods that can  
34 further distinguish spurious patches from true structures that can reveal information about time  
35 series undetected by current methods. Given the deficiencies of pointwise significance testing,  
36 there is a need to improve current methods of evaluating significance of features in the wavelet  
37 domain. The areawise test, though a substantial improvement from the pointwise test has one  
38 drawback: finding the significance level of the areawise test requires a complicated root-finding

1 algorithm, making  $p$ -values for the areawise test difficult to obtain, as it would require the repeated  
2 application of a root-finding algorithm (see Sect. 4.1 for details).

3 The remainder of the paper is organized as follows. A brief overview of wavelet analysis is  
4 presented in Sect. 2. In Sect. 3, the pointwise and areawise tests are discussed briefly. The  
5 development of the geometric test is presented in Sect. 4. In Sect. 5, ideas inspired by persistence  
6 homology (Edelsbrunner, 2010) are used to show that holes, voids of pointwise significance  
7 surrounded by regions of pointwise significance, can distinguish important structures from trivial  
8 structures, linking the geometric and topological tests. Using ideas from Sect. 4 and Sect. 5, the  
9 application of a local geometric test is presented in Sect. 6. The new methods are applied to time  
10 series of two idealized cases, which provide important benchmarks for the methods, and to indices  
11 of two prominent climate modes, El Niño/Southern Oscillation and the North Atlantic Oscillation  
12 (NAO), to illustrate, in a geophysical setting, the insights afforded by the methods.

13

## 2. Definitions

14 In wavelet analysis, a time series is decomposed into frequency and time components by  
15 convolving the time series with a wavelet function satisfying certain conditions. There are many  
16 different kinds of wavelet functions but the most widely used is the Morlet wavelet, a sine wave  
17 damped by a Gaussian envelope expressed as

$$18 \quad \psi_0(\eta) = \pi^{-1/4} e^{i\omega_0\eta} e^{-\frac{1}{2}\eta^2}, \quad (1)$$

19 where  $\psi_0$  is the Morlet wavelet,  $\omega_0$  is the dimensionless frequency, and  $\eta = s \cdot t$ , where  $s$  is the  
20 wavelet scale, and  $t$  is time (Torrence and Compo, 1998; Grinsted et al., 2004). The wavelet  
21 transform of a discrete time series  $x_n$  ( $n = 1, \dots, N$ ) is given by

$$22 \quad W_n^X(s) = \sqrt{\frac{\delta t}{s}} \sum_{n'=1}^N x_{n'} \psi_0[(n' - n) \frac{\delta t}{s}], \quad (2)$$

23 where  $\delta t$  is a uniform time step determined from the time series and  $|W_n^X(s)|^2$  is the wavelet  
24 power of a time series at scale  $s$  and time index  $n$  (Torrence and Compo, 1998; Grinsted et al.,  
25 2004). Note that for the Morlet wavelet with  $\omega_0 = 6$  the wavelet scale and the Fourier period  $\lambda$  are  
26 approximately equal ( $\lambda \approx 1.03s$ ).

27

## 3. Existing significance testing methods

28

### 3.1 Pointwise significance testing

29 For climatic time series, the significance of wavelet power can be tested against a  
30 theoretical red-noise background (Torrence and Compo, 1998). For a first-order autoregressive  
31 (Markov) process

$$32 \quad X_n = \alpha X_{n-1} + w_n \quad (3)$$

1 with lag-1 autocorrelation coefficient  $\alpha$ , Gaussian white noise  $w_n$ , and  $X_0 = 0$ , the normalized  
2 theoretical red-noise power spectrum is given by

$$P_f = \frac{1 - \alpha^2}{1 + \alpha^2 - 2\alpha \cos(2\pi f/N)} \quad (4)$$

3  
4 where  $f = 0, \dots, N/2$  is the frequency index (Gilman et al., 1963). To obtain, for example, the 5%  
5 pointwise significance level one must multiple Eq. (4) by the 95% percentile of a chi-square  
6 distribution with two degrees of freedom and divide the result by 2 to remove the degree of  
7 freedom factor (Torrence and Compo, 1998). The discrete Fourier red-noise spectrum has been  
8 shown by Torrence and Compo (1998) to be adequate in estimating the significance of local  
9 wavelet power and is thus used in this paper to estimate pointwise significance. The parameter  $\alpha$   
10 can be estimated using standards methods such as the Burg's and the Yule-Walker methods (Kay,  
11 1988; Hayes, 1996).

12 Monthly time series and normalized wavelet power spectra for the NAO index (Hurrell et  
13 al., 1995, [https://climatedataguide.ucar.edu/climate-data/hurrell-north-atlantic-oscillation-nao-](https://climatedataguide.ucar.edu/climate-data/hurrell-north-atlantic-oscillation-nao-index-station-based)  
14 [index-station-based](https://climatedataguide.ucar.edu/climate-data/hurrell-north-atlantic-oscillation-nao-index-station-based)) and the Niño 3.4 index (Trenberth 1997,  
15 [http://www.cgd.ucar.edu/cas/catalog/climind/Nino\\_3\\_3.4\\_indices.html](http://www.cgd.ucar.edu/cas/catalog/climind/Nino_3_3.4_indices.html)) are shown in Figs. 1 and  
16 2. The Niño 3.4 index data were converted to anomalies by subtracting the mean monthly values  
17 for each month from the monthly values. Note that the normalized wavelet power is the wavelet  
18 power at every time and period divided by the variance of the time series, which allows different  
19 wavelet power spectra to be readily compared. Another important feature of the wavelet power  
20 spectrum is the cone of influence, the region in which edge effects become important, or more  
21 precisely, the  $e$ -folding time of the autocorrelation for wavelet power at each scale, where the  $e$ -  
22 folding time is defined by Torrence and Compo (1998) as the point at which the wavelet power  
23 for a discontinuity at the edge drops by a factor of  $e^{-2}$ . The wavelet power spectrum of the NAO  
24 index reveals numerous time periods of enhanced variance at an array of time scales, though no  
25 preferred timescale is evident. For the Niño 3.4 index, the wavelet power spectrum detects  
26 statistically significant variance in the 16-64 month period band for the period 1960-2010. Another  
27 interesting feature emerges (labeled  $H$  in Fig. 2b): regions of no pointwise significance surrounded  
28 by regions of pointwise significance. These “holes” will turn out to be important structures in  
29 wavelet power spectra and are discussed thoroughly in Sect. 5.

### 30 **3.2 Areawise significance testing**

31 The idea behind the Maraun et al. (2007) areawise test (hereafter simply the “areawise  
32 test”) is that correlations between adjacent wavelet coefficients arising from the reproducing kernel  
33 (see Appendix A) produce continuous regions of pointwise significance that resemble the  
34 reproducing kernel. The reproducing kernel for a given analyzing wavelet represents the time-  
35 scale uncertainty, which is related to the scale and time localization properties of the analyzing  
36 wavelet. Let  $(t, s)$  denote the location of a wavelet coefficient at scale  $s$  and time  $t$ . The correlation,  
37  $C(t, s, t', s')$ , between any two wavelet coefficients located at  $(t, s)$  and  $(t', s')$  obtained from the

1 wavelet transformation of a Gaussian white process is given by the reproducing kernel moved to  
 2  $t$  and stretched to  $s$  (Maraun et al., 2007), i.e.

$$\begin{aligned}
 3 \quad C(t, s, t', s') &= \sqrt{\frac{2s's}{(s')^2 + s^2}} \exp\left\{i\omega_0 \frac{s' + s}{(s')^2 + s^2} (t' - t)\right\} \\
 4 \quad &\times \exp\left\{-\frac{1}{2} \frac{(t'-t)^2 + \omega_0^2 (s'-s)^2}{(s')^2 + s^2}\right\} \quad (5)
 \end{aligned}$$

5 (Maraun and Kurths, 2004). Thus, for significance patches generated from random fluctuations,  
 6 the typical patch area is the area of the reproducing kernel. The test can be described more formally  
 7 as follows: Let  $P_{pw}$  be the set of all pointwise significance values and define a critical area  
 8  $P_{crit}(t, s)$  as the subset of the time-scale domain for which the reproducing kernel  $K$   
 9 (corresponding to the analyzing wavelet), dilated and translated to time  $t$  and scale  $s$ , exceeds the  
 10 threshold of a critical level  $K_{crit}$ . Mathematically,  $P_{crit}(t, s)$  is given by

$$11 \quad P_{crit}(t, s) = \{(t', s') : K(t, s; t', s') > K_{crit}\}. \quad (6)$$

12 It is noted that critical area of the areawise test is not area of significance patches but the  
 13 area of the reproducing kernel at some critical level and at some scale. For a patch of pointwise  
 14 significant values, a point inside the patch is said to be areawise significant if the reproducing  
 15 kernel dilated according to the scale in question entirely fits into the patch, i.e.

$$16 \quad P_{aw} = \bigcup_{P_{crit}(t,s) \subset P_{pw}} P_{crit}(t, s), \quad (7)$$

17 where  $P_{aw}$  is the subset of pointwise significant values consisting of additionally areawise  
 18 significant wavelet power coefficients. According to the areawise test, entire significance patches  
 19 need not be areawise significant, just portions or subsets of them. That is, it is only those points  
 20 that fit inside the kernel that are deemed areawise significant. The critical area is related to  
 21 significance level of the areawise test by the following equation:

$$22 \quad 1 - \alpha_{aw} = 1 - \left\langle \frac{A_{aw}}{A_{pw}} \right\rangle, \quad (8)$$

23 where  $1 - \alpha_{aw}$  is the significance level of the areawise test,  $A_{aw}$  is the area of the areawise  
 24 significance patch,  $A_{pw}$  is the area of the pointwise significance patch, and  $\left\langle \frac{A_{aw}}{A_{pw}} \right\rangle$  is the average  
 25 ratio between the areas of area wise-significant patches and pointwise significance patches. It turns  
 26 out that the calculation of  $\alpha_{aw}$  is non-trivial, involving a root-finding algorithm that solves the  
 27 equation  $f(P_{crit}) - \alpha_{aw} = 0$  (see Sect. 4).

28 To illustrate the importance of the areawise significance test, the test was applied to the wavelet  
 29 power spectra of the NAO and Niño 3.4 index time series (Figs. 3 and 4). Numerous 5% pointwise  
 30 significance patches in the Niño 3.4 wavelet power spectrum were found to contain areawise-

1 significant subsets, suggesting that these patches were less likely to be an artifact of multiple  
 2 testing. For example, as indicated by the thick red contours, there are three areawise-significant  
 3 regions located at a period of approximately 48 months, one at 1890, one at 1905, and a third one  
 4 at 1985. Many more areawise-significant regions were identified at periods less than 8 months,  
 5 especially before 1955. The wavelet power spectrum of the NAO index also contained pointwise  
 6 significance patches with areawise-significant subsets, all at periods less than 8 months. However,  
 7 it will be shown in Sect. 4 that they all may be artifacts of multiple testing, resulting from the large  
 8 number of patches to which the areawise test was applied.

## 9 4. Geometric significance testing

### 10 4.1 Development

12 A disadvantage of the areawise test is the complexity of the  $\alpha_{aw}$  calculation, which involves a  
 13 root-finding algorithm. It is therefore desirable to construct an alternative test whose significance  
 14 level is easy to calculate, readily allowing the following: (1) the application of the test to patches  
 15 at various pointwise significance levels; (2) the adjustments of the significance level of the test;  
 16 (3) the application of the test to wavelet power spectra obtained using other analyzing wavelets;  
 17 and (4) the implementation of  $p$ -value adjustment procedures to control the family-wise error rates  
 18 and false discovery rates.

19 The development of a geometric significance test will require ideas from basic geometry and  
 20 set theory. In wavelet analysis, the wavelet power is computed at a discrete set of time coordinates  
 21  $T$  with elements  $t_i$  for  $i = 1, \dots, N$  and at a discrete set of scales  $S$  whose elements  $s_j$  ( $j=1, \dots, J$ )  
 22 are given by

$$23 \quad s_j = s_{min} s^{j\delta j} \quad (9)$$

24 and

$$25 \quad J = \delta j^{-1} \log_2 \left( \frac{N\delta t}{s_{min}} \right), \quad (10)$$

26 with  $\delta t$  a time step and  $s_{min}$  the smallest resolvable scale (Torrence and Compo, 1998). Note that  
 27 the maximum value of  $\delta j$  for which adequate sampling can be achieved depends on the wavelet  
 28 function, being approximately equal to 0.5 for the Morlet wavelet. For the geometric test, a patch  
 29 will be considered to be a polygon with vertices  $v_k = (x_k, y_k)$  for  $k = 0, \dots, m-1$ , where  $x_k$  and  $y_k$   
 30 are, respectively, elements from  $T$  and  $S$  and  $m-1$  is the number of vertices. It is worth noting that  
 31 not all patches are closed in the sense that some are located near the edges of the wavelet domain.  
 32 To remedy this problem, semi-enclosed patches are artificially closed by connecting the two  
 33 vertices located on the boundary of the wavelet domain with a line segment.



1 Perhaps the most fundamental property of a pointwise significance patch is its area, which  
 2 can be calculated using the following special case of Green's Theorem:

$$3 \quad A = \frac{1}{2} \left| \sum_{k=0}^{m-1} (x_k y_{k+1} - x_{k+1} y_k) \right|, \quad (11)$$

4 where  $y_0 = y_m$ ,  $x_0 = x_m$  (Worboys and Duckham, 2004). For significance patches containing  
 5 holes, the total area of the holes is subtracted from the area the significance patch would have if  
 6 it did not contain the holes.

7 What will be of particular interest is the normalized area of a significance patch, not its  
 8 absolute area. To compute the normalized area, the centroid of a significance patch will need to be  
 9 calculated using the following formulas (Worboys and Duckham, 2004):

$$10 \quad C_t = \frac{1}{6A} \sum_{k=0}^{m-1} (x_k + y_{k+1}) (x_k y_{k+1} - x_{k+1} y_k) \quad (12)$$

11 and

$$12 \quad C_s = \frac{1}{6A} \sum_{k=0}^{m-1} (y_k + x_{k+1}) (x_k y_{k+1} - x_{k+1} y_k), \quad (13)$$

13 where  $C_t$  and  $C_s$  are the time and scale coordinates, respectively, of the centroid. Recall that the  
 14 centroid is the area-weighted location of a polygon. If  $A_R$  is the area of the reproducing kernel  
 15 dilated or contracted (at a certain critical level) to  $(C_t, C_s)$ , then the normalized area of a significance  
 16 patch is given by

$$17 \quad A_n = \frac{A}{A_R}, \quad (14)$$

18 and allows one to compare sizes of significance patches across all scales simultaneously. Two  
 19 idealized pointwise significance patches with equal normalized area are shown in Figs. 5a and 5b.

20 The idea of the geometric significance test is to generate a null distribution of  $A_n$  and use  
 21 the null distribution to compute the significance of patches in the wavelet domain. In climate  
 22 science, a suitable null hypothesis is red-noise so that  $A_n$  will be computed for a large ensemble  
 23 of patches generated from red-noise processes. Using the null distribution of  $A_n$ , one can assign to  
 24 each patch in the wavelet domain a probability  $p$  that the patch was not generated from a random  
 25 stochastic fluctuation. It is noted that the null distribution of  $A_n$  depends on the choice of null  
 26 hypothesis (not shown), with, for red-noise processes,  $A_n$  increasing with increasing  
 27 lag-1 autocorrelation coefficients.

28 The calculation of the geometric significance level  $1 - \alpha_g$ , unlike the calculation of  
 29  $1 - \alpha_{aw}$ , is straightforward: for the areawise test one needs to compute  $\alpha_{aw}$  as a function of  $P_{crit}$ ,  
 30 whereas for the geometric test  $\alpha_g$  is no longer a function  $P_{crit}$ . Moreover, the estimation of  $P_{crit}$   
 31 involves a root-finding algorithm that solves the equation  $f(P_{crit}) - \alpha_{aw} = 0$ , where  $f(P_{crit})$  is

1 estimated using Monte Carlo simulations. Thus, the application of the areawise test to pointwise  
2 significance patches for  $M$  different values of  $\alpha_{aw}$  would require  $M$  Monte Carlo ensembles,  
3 making  $p$ -values for the test difficult to obtain. For the geometric test, only a single Monte Carlo  
4 ensemble is needed, as a single choice of  $P_{crit}$  is needed to generate a null distribution, from which  
5 any desired value of  $\alpha_g$  can be obtained. In fact, while the choice of  $P_{crit}$  impacts the mean value  
6 of the null distribution, the geometric significance of a significance patch is left unchanged, as the  
7 significance is relative to a distribution of  $A_n$  under some noise model (Appendix B).

8 The elimination of the  $P_{crit}$  dependence from the calculation of the geometric significance  
9 level allows the geometric test to be readily performed on patches of various pointwise significance  
10 levels. For the areawise test, a new  $P_{crit}$  must be estimated for each pointwise significance level  
11 since  $A_{pw}$ , on average, will change depending on if the pointwise significance level  $1 - \alpha_p$  is  
12 increased (patches shrink) or is decreased (patches grow). For the geometric test, there is no need  
13 to find a new  $P_{crit}$  —simply compute a new null distribution based solely on the information of  
14 the pointwise significance patches at some pointwise significance level  $1 - \alpha_p$ .

15 Another advantage of eliminating the  $P_{crit}$  dependence is that the geometric test can be  
16 readily applied to wavelet coherence, partial wavelet coherence (Ng, 2012), multiple wavelet  
17 coherence, and cross-wavelet spectra. The application of the geometric test to significance patches  
18 in the aforementioned wavelet spectra only requires a single Monte Carlo ensemble to generate a  
19 null distribution, eliminating the calculation of a new  $P_{crit}$  for each wavelet spectra and for each  
20 value of  $\alpha_g$ . For the areawise test, a new  $P_{crit}$  must be estimated for each value of  $\alpha_{aw}$  and for  
21 each wavelet spectra, making the areawise test difficult to implement in practical applications.

22 It may happen that a pointwise significance patch is so large that individual oscillations  
23 embedded in the patch cannot be detected by the geometric test. However, there are two solutions  
24 to this localization problem: the first solution is to increase the significance level of the pointwise  
25 test, allowing large patches to separate, and then perform the geometric test on the smaller patches.  
26 The second solution is to examine other properties of significance patches that may indicate the  
27 presence of multiple periodicities that form large significance patches from the merging of several  
28 smaller patches. The second solution will be addressed thoroughly in Sect. 5.

29 Another situation that may arise in practice is the application of the geometric test to  
30 patches located both inside and outside the cone of influence (COI). In the case of the pointwise  
31 significance test, the edge effects only influence those wavelet power coefficients that lie inside  
32 the COI; however, for the geometric test, the significance of the entire patch will be impacted even  
33 if the patch only partially lies inside the COI. The reason is that the COI will act to decrease the  
34 size of significance patches through the reduction of wavelet power in the COI and subsequently  
35 the total area of the patch. One should thus be cautious when interpreting the results of the  
36 geometric test for patches near the COI.

## 37 4.2 Multiple testing

1 If the geometric test was performed on  $K$  significance patches at the  $\alpha_{geo}$  level, then, on  
2 average, one can expect  $\alpha_{geo}K$  false positive results, which would make the geometric test  
3 permissive for large  $K$ . It is therefore necessary to reduce the number of false positive results.  
4 There are various ways to reduce the number of false positives, including the Walker test,  
5 Bonferroni correction, and other counting procedures (Wilks, 2006). Recently, methods for  
6 controlling the false discovery rate (FDR) have been developed, where the FDR is the expected  
7 proportion of rejected local null hypotheses that are actually true (Benjamini and Hochberg, 1995).  
8 In particular, Benjamini and Hochberg (1995) developed a method for controlling the FDR based  
9 on the number of local hypotheses being tested and the degree to which the local hypotheses were  
10 rejected, contrasting with other procedures that ignore the confidence with which the local tests  
11 reject the local hypotheses (Wilks, 2006). Moreover, the method has proven to have high statistical  
12 power, especially when only a small fraction of the  $K$  local tests correspond to false null hypotheses  
13 (Wilks, 2006). The procedure will therefore be used to control the false discovery rate of the  
14 geometric test, which will facilitate the interpretation of results.

15 Suppose that  $K$  local hypotheses were tested, where, in the present case, the local  
16 hypotheses refer to the testing of each patch individually under the assumption that the results of  
17 the individual tests are independent. A global geometric test can be performed at the  $\alpha_{global}$  level  
18 as follows: Let  $p_{(l)}$  denote the  $l$ th smallest of  $K$  local  $p$ -values; then, under the assumption that the  
19  $K$  local tests are independent, the FDR can be controlled at the  $q$ -level by rejecting those local tests  
20 for which  $p_{(l)}$  is no greater than

$$21 \quad p_{FDR} = \max_{r=1, \dots, K} [p_{(r)} : p_{(r)} \leq q(r/K)] \quad (15)$$

$$22 \quad \max_{r=1, \dots, K} [p_{(r)} : p_{(r)} \leq \alpha_{global}(r/K)] \quad (16)$$

23 so that the FDR level is equivalent to the global test level. According to the procedure, any local  
24 test resulting in a  $p$ -value less than or equal to the largest  $p$ -value for which Eq. (16) is satisfied is  
25 deemed significant. If no such local  $p$ -values exist, then none are deemed significant and, therefore,  
26 the global test hypothesis cannot be rejected. The global geometric test will thus only deem those  
27 significant patches with  $p$ -values satisfying Eq. (16) as significant. Throughout the paper  
28  $q = \alpha_{global}$  will be set to 0.05.

### 29 **4.3 Comparisons with the areawise test**

30 With a formal geometric significance test now developed, it is useful to compare the  
31 areawise and geometric significance tests, where comparisons will be made using an empirically  
32 derived quantity. Let  $N_{sig}$  be the number of pointwise significance patches in a given wavelet  
33 power spectrum,  $N_a$  the number of patches containing an areawise-significant region,  $N_g$  the  
34 number of geometrically significance patches, and  $N_{ag}$  the number patches that are both  
35 geometrically significant and that contain areawise-significant regions. The quantity

$$I_{sim} = \frac{N_{sig} - N_a - N_g + 2N_{ag}}{N_{sig}} \quad (17)$$

then measures the similarity between the two tests. The interpretation of  $I_{sim}$  is as follows: if  $I_{sim} = 1$  then all patches containing areawise-significant regions are also geometrically significant and all patches which do not contain areawise-significant regions are also not geometrically significant. On the other hand, for values of  $I_{sim}$  less than 1 some patches containing areawise-significant regions may not be geometrically significant, with the converse also being true.

To better compare the similarity between the two tests, distributions of  $I_{sim}$  were constructed by generating 1000 synthetic wavelet power spectra of red-noise processes with fixed autocorrelation coefficients and length  $N = 1000$  (arbitrary units) and computing  $I_{sim}$  for each of the synthetic wavelet power spectra. The experiment was performed for red-noise processes with different lag-1 autocorrelation coefficients to determine if  $I_{sim}$  depends on the AR1 model. The results are shown Fig. 6a. With a mean value of 0.90, a strong agreement was found between the areawise and geometric tests, differences arising from the fact that the areawise test is a local test, finding significant regions within patches, whereas the geometric test assigns a significance value to entire patches (see discussion below). Since  $I_{sim}$  was often less than 1.0, some patches containing areawise-significant regions were not found to be geometrically significant, and, conversely, some patches were geometrically significant without containing areawise-significant regions.

The quantity  $r_{neg} = N_g/N_a$ , which measures the ratio of false positive results between both tests, was also computed for case when both the geometric and areawise test levels were set to 0.05 (Fig. 6b). In this case, the mean value of  $r_{neg}$  was found to range from 1.0 to 2 and the median value was found to be generally greater than 1.0, ranging from 1 to 1.8. No dependence on the lag-1 autocorrelation coefficients was identified. The results indicate that the geometric test is generally less conservative than the areawise test for a given wavelet power spectrum. The lack of conservativeness, however, can be remedied by controlling the FDR of the geometric test at the  $q = 0.05$  level. Fig. 6b shows  $r_{adj}$ , the ratio of false positive results between the areawise tests and the geometric test but with FDR controlled for the geometric test. As indicated in Fig. 6b, by controlling the FDR the geometric test is much more conservative than the areawise test, resulting in fewer false positive results, with a typical value of  $r_{adj}$  ranging from 0.02 to 0.05.

To explain the differences between the areawise and geometric tests, it will be necessary to consider the convexity of a patch, the degree to which a polygon or point set lacks concavities. The reason for considering convexity is illustrated by considering the two significance patches shown Fig. 5, which have equal values of  $A_n$  but different geometries: one is convex (i.e., has no concavities, Fig. 5a) and the other is not convex (Fig. 5b). Suppose that the areawise test was performed on the two patches at the  $\alpha_{aw}$  level. For the convex patch shown Fig. 5a, the reproducing kernel is capable of fitting entirely inside the patch but is unable to fit inside the non-convex patch as a result of the concavity. Thus, although having equal area, the two patches differ

1 in their areawise significance, where the difference in significance is related to their geometry.  
2 Thus,  $p_{aw} = g(\mathcal{C}, A; H_0)$  for some function  $g$ , where  $p_{aw}$  is the areawise test  $p$ -value associated  
3 with a patch calculated under the null hypothesis  $H_0$  and  $\mathcal{C}$  is the convexity of the patch, which is  
4 now formally defined.

5 Rigorously, convexity is defined as follows: Let  $x$  and  $y$  be any two points in a set  $Z$ ; then  
6 the set  $Z$  is convex if for all  $t$  the line segment

$$7 \quad [x, y] = \{tx + (1 - t)y : 0 \leq t \leq 1\} \quad (18)$$

8 is in  $Z$  (Ziegler, 1995). Equivalently, a set is convex if it contains any line segment joining any  
9 pair of points in  $Z$ . Under this definition, for example, patches with thin bridges as described by  
10 Maraun et al. (2007) are not convex.

11 To quantify convexity, another idea from set theory, the convex hull, will be needed, which  
12 for a point set  $Z$  is defined as the intersection of all convex sets containing  $Z$  (Ziegler, 1995). In  
13 other words, it is the smallest convex set containing  $Z$  constructed from the intersection of all  
14 convex sets containing  $Z$ . Mathematically, the convex hull of a point set  $Z$  is expressed as

$$15 \quad \text{conv}(Z) = \bigcap \{Z' \subseteq \mathbb{R}^2 : Z \subseteq Z', Z' \text{ convex}\}. \quad (19)$$

16 In practical applications, the convex hull of a set can be easily computed using existing algorithms  
17 (Barber et al., 1996). It is noted that all holes are ignored in the computation of the convex hull  
18 because the computation of the convex hull assumes that there are no holes in the polygon. A  
19 patch containing a hole can never have a smallest convex set containing the set because holes allow  
20 line segments to leave the patch regardless of the size of the convex hull.

21 A metric for convexity will now be defined using the area of a significance patch together  
22 with the area of its convex hull as follows: If  $A_k$  is the area of the convex hull of a significance  
23 patch whose area is  $A$ , then the convexity is

$$24 \quad \mathcal{C} = \frac{A}{A_k}, \quad (20)$$

25 where  $0 \leq \mathcal{C} \leq 1$ . High values of  $\mathcal{C}$  correspond to significance patches with relatively small  
26 concavities, whereas small values of  $\mathcal{C}$  correspond to patches with relatively large concavities, as  
27 in the case of significance patches with thin bridges.

28 According to the areawise test, patches with smaller values of  $\mathcal{C}$  are less likely to be  
29 areawise significant so that it is expected that patches deemed significant by the areawise test will  
30 be primarily convex. To test this hypothesis, 10,000 patches arising from red-noise processes with  
31 different lag-1 autocorrelation coefficients were generated and the convexity of those patches  
32 deemed areawise significant at the  $\alpha_{aw} = 0.05$  level was calculated. The results in Fig. 6c show  
33 the mean convexity as a function of the lag-1 autocorrelation coefficients, together with the 95%

1 confidence bound. The mean convexity of the patches was found to be approximately 0.8,  
2 regardless of the lag-1 autocorrelation coefficient. An identical experiment was also performed for  
3 geometrically significant patches but with the convexity of patches that are geometrically  
4 significant at the  $\alpha_{geo} = 0.05$  being computed. In contrast to areawise-significant patches, patches  
5 that were found to be geometrically significant, on average, had lower convexity, the reason for  
6 which is that the calculation of  $\alpha_{geo}$  makes no assumption about convexity. The  $p$ -value for the  
7 geometric test is thus  $p_{geo} = f(A; H_0)$  for some function  $f$ , contrasting with  $p_{aw}$  that depends on  
8 convexity. The results of the experiments are consistent with Figs. 5a and 5b, where both the ideal  
9 patches have the same geometric significance but the ideal patch in Fig. 5b has a larger  $p_{aw}$  so that  
10  $p_{aw} > p_{geo}$ .

11 Convexity cannot fully explain the differences between  $p_{aw}$  and  $p_{geo}$  for a given patch.  
12 More generally,  $p_{aw} = g(\mathcal{C}, A, S_1, \dots, S_R; H_0)$ , where  $S_1$  to  $S_R$  are shape parameters of the patch,  
13 such as aspect ratio and symmetry. Consider, for example, a convex patch whose length in the time  
14 direction is long with respect to the reproducing kernel (at some critical level) but thin in the scale  
15 direction with respect to the reproducing kernel. Such a patch would be deemed insignificant by  
16 the areawise test, though it may have an area much larger than the critical area of the areawise test.  
17 Asymmetry with respect to the scale axis, as another example, may also result in a patch being  
18 deemed insignificant by the areawise test if, for example, the width of the patch in the scale  
19 direction decreases with time. If the normalized areas of such patches are larger than the critical  
20 level of the geometric test, the patches will be geometrically significant, though may not be  
21 areawise significant if the reproducing kernel is unable to fit inside the narrow portion of the patch.  
22 The above arguments suggest that  $f(A; H_0) \neq g(\mathcal{C}, A, S_1, \dots, S_R; H_0)$  and thus the significance of  
23 patches as determined by the geometric and areawise tests need not be equal.

#### 24 **4.4 Geometric significance testing of climatic data**

26 For climatic time series, significance is often tested against a red-noise background and  
27 therefore it is reasonable to expect that the areawise and geometric tests behave similarly when  
28 applied to climatic time series. As such, the areawise and geometric tests were applied to the NAO  
29 and Niño 3.4 time series. For the wavelet power spectrum of the NAO index time series (see Fig.  
30 3), not a single patch was found to be geometrically significant after controlling the FDR at the  
31 0.05 level, suggesting the NAO index time series is composed of stochastic fluctuations. In fact,  
32 the NAO has already been shown to be consistent with a first-order Markov process (Feldstein,  
33 2002). Recent work by Hanna et al. (2014) claimed that the NAO variability has increased over  
34 the past 30 years; however, the results from this analysis suggest that such changes cannot be  
35 distinguished from stochastic fluctuations, which could render difficult projections of future  
36 changes of the NAO.

37 The wavelet power spectrum of the Niño 3.4 index (see Fig. 4) was found to contain numerous  
38 geometrically significant patches in the period band 16-64 months, especially after 1960. The 5%  
39 pointwise significance patch extending from 1980 to 2000, as an example, was found to be

1 significant, as well as the patch centered at 2008. The significance patch centered at 1985 and at  
2 a period of 32 months, however, is so large that individual oscillations could not be identified. To  
3 remedy the problem, the geometric significance was applied to 1% ( $\alpha_p = 0.01$ ) pointwise  
4 significance patches with  $q = 0.05$ , resulting in 1% pointwise significance patches at 1970, 1995,  
5 and 2007 being deemed significant, all of which also contained areawise-significant regions.  
6 Patches located at a period less than 8 months were also found to be geometrically significant,  
7 though only before 1955.

## 8 **5. Topological significance testing**

### 9 **5.1 Topological significance testing of ideal time series**

10 Topology is a branch of mathematics concerned with properties of spaces that remain  
11 unchanged after continuous deformations. So far only geometric aspects of significance patches  
12 have been discussed. Area of a significance patch, as an example, is a geometric property in the  
13 sense that stretching the patch in both the scale and time direction would increase its area. There  
14 are properties, however, that would be unaffected by stretching the significance patch. As a  
15 motivating example, consider the significance patches shown in Fig. 4 corresponding to the  
16 wavelet power spectrum of the Niño 3.4 index (see Fig. 2), where there is a hole or void of  
17 pointwise significance located within a significance patch at 1985. This feature is topological, as  
18 the hole would remain under a continuous deformation such as stretching. A more formal  
19 definition of a hole will require some notions from topology. Let  $I = [0,1]$  be the closed unit  
20 interval. Then a path from a point  $a$  to a point  $b$  in a significance patch  $P$  is a continuous function  
21  $f: I \rightarrow P$  with  $f(0) = a$  and  $f(1) = b$ , where in the case that  $f(0) = f(1) = c$  the path is said to be closed  
22 (Hatcher, 2002). Note that a point is a special kind of closed path called the constant path. A patch  
23 will be said to contain a hole if there exists a path in the significance patch such that it cannot be  
24 continuously deformed into a point, where the feature obstructing the path from such a deformation  
25 is a hole. The definition is consistent with notions of simply-connectedness in topology (Hatcher,  
26 2002). Figure 4 shows an example of a closed path (blue curve) in a patch that cannot be contracted  
27 to a point because it surrounds a hole located in the patch.

28 For a patch with a hole, there will be two boundaries, an external boundary and an internal  
29 boundary representing the boundary between the hole and the patch. Thus, if a patch contains an  
30 internal boundary or contour it will contain a hole, whereas a patch without a hole will contain no  
31 internal contours. In practical applications, the existence of a hole can be determined by orienting  
32 external contours in the clockwise direction and internal contours in the counter-clockwise  
33 direction, a procedure automatically implemented by the Matlab contour routine. The number of  
34 counter-clockwise oriented contours is thus the number of holes in the wavelet power spectrum at  
35 a given pointwise significance level.

36 To begin the topological analysis, the topology of time series with known structures will be  
37 analyzed. Given the importance of red-noise processes in the spectral analysis of climatic time

1 series, the topology of patches generated from red-noise processes is first considered to determine  
 2 if pointwise significance patches can be distinguished from those generated from red-noise  
 3 processes solely based on their topology. To answer this question, 10,000 wavelet power spectra  
 4 of red-noise processes were generated and the number of holes (denoted by  $N_h$  hereafter) at a finite  
 5 set of pointwise significance levels was computed for each wavelet power spectra (Fig. 7). It was  
 6 found that  $N_h$  is not a random function of the pointwise significance level, as indicated by the 95%  
 7 confidence bounds. Most importantly, for pointwise significance levels less than 10%, few patches  
 8 contained holes, suggesting that holes are an uncommon feature of significance patches generated  
 9 from red-noise processes (Table 1) and therefore can be used to distinguish spurious patches from  
 10 important structures. It also noted that neither the shape nor the amplitude of the curve in Fig. 7  
 11 depends on the lag-1 autocorrelation coefficient of the red-noise process. Table 1 also suggests  
 12 that patches containing more than a single hole are unlikely to be the result of red-noise, even for  
 13 a modest pointwise significance level of 20%. For pointwise significance levels of 1% and 5%,  
 14 no more than a single hole was identified in a given patch.

15 A simple algorithm for assessing the significance of holes is therefore developed. To find the  
 16 significance of holes, plot the centroids of holes at a finite set of pointwise significance levels and  
 17 project the centroids onto the wavelet domain, resulting in a topological wavelet diagram. The  
 18 number of holes contained in a patch should also be computed, as patches with more holes are less  
 19 likely to result from red-noise. In accordance with Fig. 7 and Table 1, regions in the wavelet  
 20 domain where holes exist below the 20% pointwise significance level will be considered regions  
 21 with significant topological features.

22 With a method for assessing the significance of holes, it is reasonable to analyze different  
 23 ideal time series, both linear and nonlinear, to determine what types of time series produce holes  
 24 in significance patches. Perhaps the simplest case is a single sinusoid with additive white noise  
 25 (not shown), where the time series power spectrum is tested against a white-noise background  
 26 spectrum. In this case, no evidence was found that a single sine wave, regardless of amplitude and  
 27 signal-to-noise ratio, is capable of generating holes in 5% pointwise significance patches. A similar  
 28 experiment was repeated but the power spectra of the sine waves were tested against red-noise  
 29 spectra. The results also indicated that a single sine wave is incapable of producing holes in 5%  
 30 pointwise significance patches, implying holes arise from a richer structure embedded in time  
 31 series. Thus, two more complex cases are considered.

32 To derive the Case 1 time series, first consider the nonlinear system

$$33 \quad X_{out}(t) = bX_{in}(t) + \gamma X_{in}^2(t), \quad (21)$$

34 where  $X_{in}(t)$  is the input into the system,  $X_{out}(t)$  is the output of the system,  $b$  is a linear  
 35 coefficient, and  $\gamma$  is a nonlinear coefficient. The output from this system will be quadratically  
 36 phased coupled (King, 1996), where quadratic phase coupling indicates that for frequencies  $f_1, f_2,$



1 and  $f_3$  and corresponding phases  $\phi_1$ ,  $\phi_2$ , and  $\phi_3$  the sum rules  $f_1 + f_2 = f_3$  and  $\phi_1 + \phi_2 = \phi_3$   
 2 are satisfied. In Case 1,  $X_{in} = \cos 2\pi ft$  so that

$$3 \quad X_{out}(t) = \frac{\gamma}{2} + b \cos 2\pi ft - \frac{\gamma}{2} \cos 4\pi ft, \quad (22)$$

4 indicating that the output contains an additional frequency component at the harmonic  $2f$   
 5 (harmonic generation) and the mean value of the output has shifted (rectification) with respect to  
 6 the input. Figures 8a and 8b show the time series of  $X_{out}$  and the significance of the wavelet power  
 7 for the case when  $f = 1/64 = 1/\lambda_1$ ,  $b = 1$ ,  $\phi_1 = \pi/2$ ,  $\phi_2 = \pi/3$ , and  $\gamma = 0.25$  (arbitrary units)  
 8 and with Gaussian white noise added to the output. In this case, the significance of the wavelet  
 9 power was tested against a red-noise background spectrum. Figure 8 shows numerous pointwise  
 10 significance patches, all of which are spurious except for the one at  $\lambda_1 = 64$ . The areawise and  
 11 geometric test correctly identified the pointwise significance patch at  $\lambda_1 = 64$  to be significant but  
 12 deemed a spurious patch as significant at time 140 and at  $\lambda = 3$ . It is noted that -the geometric test  
 13 only deemed the 1% pointwise significance patch at  $\lambda_1 = 64$  as significant. Also note that the  
 14 pointwise significance test was unable to detect the harmonic with period  $\lambda_2 = 32$  using a red-  
 15 noise background spectrum.

16 It should be noted, however, that if the parameter  $\gamma$  were increased to a value greater than  
 17 1, the oscillation with period  $\lambda_2 = 32$  would become more prominent. In fact, it was found that  
 18 for  $\gamma \geq 1$  the areawise and geometric tests perform better (not shown), correctly identifying the  
 19 oscillation with period  $\lambda_2 = 32$ , with the result also depending on the noise level of the white  
 20 noise. Case 1 thus only serves as an illustrative example of a situation that may arise when a  
 21 wavelet analysis is applied to a geophysical (often noisy) time series.

22 To extract more information from the wavelet power spectrum, the centroids of holes were  
 23 plotted as a function of the pointwise significance level (Fig. 8c). Figure 8c shows that holes only  
 24 existed at pointwise significance levels of at most 15% and 20% and therefore not all nonlinear  
 25 time series can generate holes at the 5% pointwise significance level, suggesting that the relative  
 26 difference between the primary frequency components or the resulting frequency combinations is  
 27 important, as discussed below. The amplitudes of the coefficients  $b$  and  $\gamma$ , as well as the signal-to-  
 28 noise ratio of the Gaussian white noise, turn out to be also important, which is discussed below.

29 Case 2 is the quadratically phase-coupled time series

$$30 \quad X(t) = a \cos(2\pi f_1 t + \phi_1) + b \cos(2\pi f_2 t + \phi_2) +$$

$$31 \quad \gamma \cos[2\pi(f_1 + f_2)t + \phi_1 + \phi_2], \quad (23)$$

32 which consists of three frequency components:  $f_1 = 1/20 = 1/\lambda_1$ ,  $f_2 = 1/30 = 1/\lambda_2$ , and  
 33  $f_1 + f_2 = 1/12 = 1/\lambda_3$ , and  $\gamma$  is assumed to be 0.5. It is noted that Case 1 is a special case of  
 34 Case 2. Like Case 1, wavelet power was also tested against a red-noise background. Unlike the  
 35 significance patches in Fig. 8c corresponding to Case 1, holes have appeared in 5% pointwise

1 significance patches between periods  $\lambda_1 = 20$  and  $\lambda_2 = 30$  (Fig. 9b). Moreover, the 5% pointwise  
2 significance patch containing the hole (labeled  $P_1$ ) was found to be geometrically significant but  
3 was not found to contain an areawise-significant subset. It is also worth noting that the areawise  
4 and geometric tests failed to detect a significant periodicity at  $\lambda_1 = 20$  despite the fact that it is  
5 known to exist by construction. Figure 9c shows that a few holes existed at low pointwise  
6 significant levels ( $\leq 20\%$ ), though only one was found at the 5% pointwise significance level (light  
7 red shading). However, if one applies the pointwise significance test to the wavelet power at the  
8 20% significance level a feature emerges that can hardly be produced from red-noise (see Table  
9 1), namely a large 20% significance patch (light blue shading) containing four holes located in the  
10 period band 20-30. One can thus have confidence that the feature is significant. Furthermore, by  
11 constructing a patch topologically unlike those generated from red-noise, significant wavelet  
12 power extending from time 20 to 300, undetected by the pointwise, areawise, and geometric tests,  
13 has been recovered, whereas only applying the 5% pointwise test would result in two patches that  
14 are seemingly indistinguishable from red-noise (labeled  $P_2$  and  $P_3$ ), with only one at  $\lambda_2 = 30$   
15 being geometrically significant.

16 The ability of the pointwise, areawise, and geometric tests to detect significant structures  
17 inevitably depends on the parameters  $a, b, \gamma, f_1$ , and  $f_2$ . In fact, Maruan et al. (2007) has already  
18 determined that the pointwise test and areawise test are sensitive to the signal-to-noise level. It was  
19 hypothesized that the results of the topological method also depend on the parameters  $a, b, \gamma, f_1$ ,  
20 and  $f_2$ . To test the hypothesis, several experiments were performed, the first of which investigated  
21 the relationship between  $f_1, f_2$ , and the number of holes. The experiment is described below.

22 Though both ideal time series contain a quadratic nonlinearity, the nonlinear interaction in  
23 Case 2 contained oscillations with nearby frequency components, allowing the formation of holes,  
24 whereas for Case 1 no significant holes appeared in significance patches. It appears that the  
25 presence of holes depends on the relative location of two oscillations in the frequency domain, and  
26 thus it is reasonable to suspect that there exists a critical frequency difference  $\Delta f_{crit}$ , measuring  
27 the maximum frequency difference for which holes will appear in a wavelet power spectrum. An  
28 empirically derived  $\Delta f_{crit}$  was determined by generating a large ensemble of time series of the  
29 form

$$30 \quad x(t) = \cos 2\pi f_1 t + \cos 2\pi f_2 t + w(t), \quad (24)$$

31 where  $f_2 > f_1 > 0$  were generated at random,  $w(t)$  is additive white noise, and all the time series  
32 were of a fixed length. The signal-to-noise ratio was fixed to 20 and each wavelet power spectrum  
33 was tested against a red-noise background spectrum. Figure 10 shows the mean value of  $N_h$  as a  
34 function of  $\Delta r = (f_2 - f_1)/f_2$ , the relative fractional change. For  $\Delta r = 0.5$ , holes never appeared,  
35 whereas for  $\Delta r = 0.3$  holes appeared frequently. There is therefore a preferred frequency  
36 combination for which holes are more likely to appear. It was estimated that the upper critical  
37 value of  $\Delta r$  is  $\Delta r_{crit} = 0.45$ . Using the definition of  $\Delta r$ , one can write  $\Delta f_{crit} = 0.45 f_2$  and therefore  
38 the critical frequency difference is a function of  $f_2$ .

1        It turns out that even if the above experiment (not shown) was repeated using white-noise  
2 rather than red-noise background spectra  $\Delta r_{crit}$  would still be equal to 0.45, though more holes  
3 were found to appear at signal-to-noise ratios less than 2. It was expected, however, that  $\Delta r_{crit}$   
4 also depends on the amplitudes of the cosines in Eq. 24. Thus, a third experiment was conducted  
5 in which the amplitudes of the cosines were allowed to vary from 1 to 50 and  $f_1$  and  $f_2$  were  
6 allowed to vary from 0 to 0.5. The experiment was repeated for signal-to-noise ratios from 1 to 20.  
7 The results from the experiments (not shown) indicate that for red-noise background spectra and  
8 for a signal-to-noise ratio of 20 that  $\Delta r_{crit} = 0.53$ , contrasting with the case for white-noise  
9 background spectra where  $\Delta r_{crit}$  was found to be 0.51.

10        The empirical results shown in Fig. 10 have theoretical implications. Suppose that a time  
11 series contained two oscillations of equal amplitude such that frequency components of the two  
12 oscillations were such that  $f_2 = 2f_1$ . Furthermore, suppose that the wavelet power of the  
13 oscillations were computed and the significance was tested against a red-noise or white-noise  
14 background spectrum. In this case,  $\Delta r = 0.45$  and therefore holes will almost never appear in 5%  
15 pointwise significance patches, making the detection of quadratic phase coupling using topological  
16 methods more difficult in the case of self-interactions. More generally, suppose that a single  
17 sinusoid  $X_{in}(t) = \cos 2\pi f t$  is passed through the nonlinear system

$$18 \quad X_{out}(t) = bX_{in}(t) + \gamma X_{in}^{2n}(t), \quad (25)$$

19 where, after using the power-reduction for a cosine (Beyer, 1987), the output is given by

$$20 \quad X_{out}(t) = b \cos 2\pi f t + \frac{\gamma}{2^{2n}} \binom{2n}{n} + \frac{\gamma}{2^{2n-1}} \sum_{k=0}^{n-1} \binom{2n}{k} \cos 4\pi f(n-k)t, \quad (26)$$

21 where  $n$  is a positive integer and  $\binom{n}{q}$  is a binomial coefficient. For the cosines in the summation,  
22 the frequency difference between any two cosines is

$$23 \quad \Delta f = 4\pi f(n-p) - 4\pi f(n-m) = 4\pi f(m-p), \quad (27)$$

24 where  $0 \leq p < m \leq n-1$ . Thus,

$$25 \quad \Delta r = (f_2 - f_1)/f_2 = \frac{4\pi f(m-p)}{4\pi f(n-p)} = \frac{m-p}{n-p}. \quad (28)$$

26 Using the fact that holes can only appear between oscillation pairs with  $\Delta r \leq 0.53$  for a red-noise  
27 background spectrum, one can show that for large  $n$  more holes are able to appear in wavelet power  
28 spectra, with the likelihood of holes appearing depending on  $b$  and  $\gamma$ , with larger values of  $b$  and  
29  $\gamma$  producing more holes. In this case, holes can form in the wavelet spectrum since, for example,  
30 if  $m = 6$  and  $p = 5$  with  $n = 10$  the condition  $\Delta r \leq 0.53$  will be satisfied. The result also holds if  
31 the order of the nonlinear interaction was odd and if the cosine function  $X_{in}(t)$  was replaced by a  
32 sine function. For an odd order nonlinear interaction, however,  $\Delta r = (2m - 2p)/(2n + 1 - 2p)$ ,  
33 where  $0 \leq p < m \leq n$ .

## 5.2 Topological significance testing of climatic time series

With a better understanding of the origins of holes contained in significance patches, the wavelet power spectra shown in Figs. 1 and 2 are now analyzed more closely. Shown in Fig. 11a is the topological wavelet diagram corresponding to the wavelet power spectrum of the Niño 3.4 index, which shows the existence of numerous holes at low ( $\leq 20\%$ ) pointwise significance levels, indicating that these patches are significant features (see Table 1). For example, the rather large patch extending from 1960 to 2013 in the period band 16 to 64 months contains a hole located at 1985 and at a period of 32 months that existed at the 5% pointwise significance level. In the same patch, three more holes existed at the 10% pointwise significance level, one located at 1975 and at a period of 48 months, a second one located at 1995 and at a period of 64 months, and a third one located at 2008 and at a period of 24 months. According to Table 1, three holes in a single 10% pointwise significance patch under the null hypothesis of red-noise is extremely unlikely, if not impossible. One can thus conclude with high confidence that the patch was not generated from a random stochastic fluctuation. Moreover, the discussion in Sect. 5.1 suggests that at the very least phase-coherent oscillations were likely present in the Niño 3.4 time series, where phase coherency implies that two oscillations have a stable relative phase relationship but are not necessarily interacting nonlinearly.

The wavelet topological diagram (Fig. 11b) corresponding to the wavelet power spectrum of the NAO is less interesting, containing few holes at high pointwise significance levels. At 1875, however, a patch contained holes at the 10% pointwise significance level, suggesting that the patch is a significant feature.

## 7. Summary and Discussion

A geometric significance test was developed for more rigorously assessing the significance of features in the wavelet domain. The geometric test, although related to the existing areawise test, was found to be more flexible in the sense that  $p$ -values could be readily calculated, involving a single Monte Carlo ensemble. Another strength of the geometric test is that the false discovery rate can be controlled at a desired level, minimizing the number of false rejections of the null hypothesis. On the other hand, the geometric test had the disadvantage of being less local than the areawise test.

It is noted that the geometric test was only applied to patches arising from the convolution of the Morlet wavelet with a time series. The results presented in this paper are not valid for wavelet power spectra obtained using other analyzing wavelets, the reason for which is that each wavelet function has different time- and scale-localization properties that inevitably impact the geometry of patches. For example, patches found in the wavelet power spectrum obtained using a Paul wavelet are elongated in the scale direction relative to those obtained using a Morlet wavelet with  $\omega_0 = 6$ , resulting in nearby patches at different scales merging together. The merging of patches

1 at different scales will alter their geometry with respect to the relatively thin (in scale) patches  
2 obtained using the Morlet wavelet.

3 One disadvantage of the geometric and areawise tests is that they require a binary decision in  
4 which pointwise and geometric significance levels must be chosen. The binary decision can be  
5 circumvented by applying a  $p$ -value adjustment procedure to the wavelet power coefficients  
6 directly. For example, one could apply the Benjamini and Hochberg (1995) procedure to the  
7 wavelet power coefficients or a modified version of the procedure developed by Benjamini and  
8 Yekutieli (2002), which is valid for any dependency structure among the local test statistics. The  
9 latter procedure would seem most appropriate given the autocorrelation structure of wavelet power  
10 coefficients; however, it is noted that the procedure has less statistical power than the original  
11 procedure valid for independent local test statistics, though Wilks (2006) found the Benjamini and  
12 Hochberg (1995) procedure to remain powerful even when the assumption of independence is  
13 violated.

14  
15 The topology of significant patches was also analyzed. Holes in significant patches, a  
16 topological notion, were capable of distinguishing spurious patches from true structures. The holes  
17 were identified as arising from phase-coherent oscillations with nearby frequency components and  
18 may indicate the existence of a nonlinear interaction. Patches arising from different analyzing  
19 wavelets can differ topologically. For the Paul wavelet, the shrinking of patches in time, for  
20 example, was found, after a preliminary investigation, to reduce the number of holes in wavelet  
21 power spectra. The reduction in the number of holes can be attributed to the tearing of a patch in  
22 the time direction. The results, however, require further investigation and are a subject of future  
23 work.

24 The new methods introduced in this paper were applied to the NAO and Niño 3.4 indices, two  
25 well-known but contrasting time series. For the Nino 3.4 index, the methods detected  
26 geometrically significant structures as well as topological structures unlike that of red-noise, which  
27 provide evidence of some predictability of El Niño/Southern Oscillation, which has become of  
28 increasing importance in climate science given that its future state is uncertain under a changing  
29 global climate system (Latif and Keenlyside, 2008). For the NAO index, the new methods were  
30 unable to detect features that are distinguishable from background noise, suggesting that the NAO  
31 is a stochastic process with little predictability. The methods developed in this paper will give  
32 researchers the tools needed for a better understanding of features found in wavelet power spectra.

33

34

35

36

37

1 **Appendix A**

2 Let  $F(s, t)$  be the continuous wavelet transform of a function  $f(t)$  such that

3 
$$F(s, t) = \iint K(s, t; s', t'')F(s', t'')ds'dt''. \quad (A1)$$

4 Then the reproducing kernel is given by

5 
$$K = \frac{1}{C_\psi \sqrt{s \alpha s' \alpha'^{5/2}}} \int \left[ \psi \left( \frac{t' - t''}{s'} \right) \psi^* \left( \frac{t - t''}{s} \right) \right] dt', \quad (A2)$$

6 where

7 
$$C_\psi = \int_0^\infty \frac{|\Psi(\omega)|^2}{\omega} d\omega < \infty, \quad (A3)$$

8 and  $\Psi(\omega)$  is the Fourier transform of the wavelet  $\psi$ , and the asterisk denotes the complex  
9 conjugate. The reproducing kernel captures the structure of wavelet coefficients whereby the  
10 wavelet coefficient at any point contains information about a nearby wavelet coefficient weighted  
11 by  $K$  (Tropea, 2007).

12

1 **Appendix B**

2 Let  $A_{patch}^N(C_t, C_s)$  be the test statistic associated with a significance patch whose centroid is  
3  $(C_t, C_s)$  and let  $A_{\alpha_g}^N$  be the value of the test statistic corresponding to the  $1 - \alpha_g$  significance level  
4 of the geometric test. Writing

5 
$$A_{\alpha_g}^N = \frac{A_{\alpha_g}}{A_R} \tag{B1}$$

6 and

7 
$$A_{patch}^N(C_t, C_s) = \frac{A_{patch}}{A_R}, \tag{B2}$$

8 it follows that

9 
$$\frac{A_{patch}^N(C_t, C_s)}{A_{\alpha_g}^N} = \frac{A_{patch}}{A_{\alpha_g}}, \tag{B3}$$

10 where  $A_{patch}$  is the area of the significance patch and  $A_{\alpha_g}$  is the area of a typical patch under  
11 the null hypothesis corresponding to the  $1 - \alpha_g$  significance level. Since Eq. (B3) no longer  
12 contains  $A_R$ , the relationship between  $A_{patch}^N(C_t, C_s)$  and  $A_{\alpha_g}^N$  no longer depends on  $P_{crit}$ .

13

14

1 **Appendix C**

2 Recall that Green's Theorem in the plane states that

3 
$$\int_C^f (Pdx + Qdy) = \iint_D^d \left( \frac{\partial Q}{\partial x} - \frac{\partial P}{\partial y} \right) dA, \text{_____} \quad (C1)$$

4 where  $C$  is a positively oriented, piecewise smooth curve, bounding a region  $D$ ,  $F = \langle P, Q \rangle$  is a  
 5 vector field on  $D$ , and  $x$  and  $y$  are the usual Cartesian coordinates (Baxandall and Liebeck, 2008).

6 Note that if one sets

7 
$$\frac{\partial Q}{\partial x} - \frac{\partial P}{\partial y} = 1, \text{_____} \quad (C2)$$

8 then the right-hand side of Eq. (C1) can be used to calculate the area of a region  $D$ . Thus, let  $Q =$   
 9  $x/2$  and  $P = -y/2$  so that

10 
$$\frac{1}{2} \int_C^f xdy - ydx = A(D), \text{_____} \quad (C3)$$

11 where  $A(D)$  denotes the area of  $D$ . Let  $(x_0, y_0), \dots, (x_{m-1}, y_{m-1})$  be  $m-1$  vertices of a polygon. If  
 12  $C_0$  is a line segment from  $(x_0, y_0)$  to  $(x_1, y_1)$ , then

13 
$$\int_{C_0}^f xdy - ydx = x_0 y_1 - x_1 y_0. \text{_____} \quad (C4)$$

14 More generally, denote by  $C_k$  the segment from  $(x_k, y_k)$  to  $(x_{k+1}, y_{k+1})$ , recalling that  $x_m = x_0$   
 15 and  $y_m = y_0$ . Since  $C = C_0 \cup C_1, \dots, \cup C_{m-1}$ , we can write

16 
$$A(D) = \frac{1}{2} \int_C^f xdy - ydx$$
  
 17 
$$= \frac{1}{2} \int_{C_0}^f xdy - ydx + \frac{1}{2} \int_{C_1}^f xdy - ydx + \dots + \frac{1}{2} \int_{C_{m-1}}^f xdy - ydx \text{_____} \quad (C5)$$

18 and thus

19 
$$A(D) = \frac{1}{2} (x_0 y_1 - x_1 y_0) + \frac{1}{2} (x_1 y_2 - x_2 y_1) + \dots + \frac{1}{2} (x_{m-1} y_0 - x_0 y_{m-1})$$
  
 20 
$$= \frac{1}{2} \sum_{k=0}^{m-1} (x_k y_{k+1} - x_{k+1} y_k). \text{_____} \quad (C6)$$



1

## 2 **References**

3 Benjamini, Y. and Hochberg, Y.: Controlling the False Discovery Rate: A Practical and Power  
4 Approach to Multiple Testing, *J. Roy. Stat. Soc.*, 57, 289-300, 1995.

5 Benjamini, Y. and Yekutieli, D.: The Control of the False Discovery Rate in Multiple Testing  
6 under Dependency, *Ann. Stat.*, 29, 1165–1188, 2001.

7 Barber, C. B., Dobkin, D. P., and Huhdanpaa, H.: Quickhull Algorithm for Convex Hulls. *ACM*  
8 *T. Math. Software*, 22, 469-483, 1996.

9 Baxandall, P. and Liebeck, H.: *Vector Calculus*, Dover Publications, INC., Mineola, New York,  
10 550 [pp.](#), 2008.

11 Beyer, W. H.: *CRC Standard Mathematical Tables*. 28<sup>th</sup> Ed. CRC Press, Boca Raton, Florida,  
12 674 [pp.](#), 1987.

13 Edelsbrunner, H. and Harer, J.: *Persistent Homology – A Survey*, *Cotemp. Math.*, 12, 1-26,  
14 2010.

15 Feldstein, S. B.: The Time Scale, Power Spectra, and Climate Noise Properties of  
16 Teleconnection Patterns, *J. Climatol.*, 13, 4430-4440, 2000.

17 Gilman, D. L., Fuglister, F. J., and Mitchell J. M. Jr.: On the Power Spectrum of “Red Noise”, *J.*  
18 *Atmos. Sci.*, 20, 182–184, 1963.

19 Grinsted, A., Moore, J. C. and Jevrejeva, S.: Application of the Cross Wavelet Transform and  
20 Wavelet Coherence to Geophysical Time Series. *Nonlinear Process. Geophys.*, 11, 561–566,  
21 2004.

22 Hasselmann, K.: *Stochastic Climate Models Part I. Theory*, *Tellus*, 28, 473-485, 1976.

23 Hatcher, A.: *Algebraic Topology*, Cambridge University Press, New York, 544 [pp.](#), 2001.

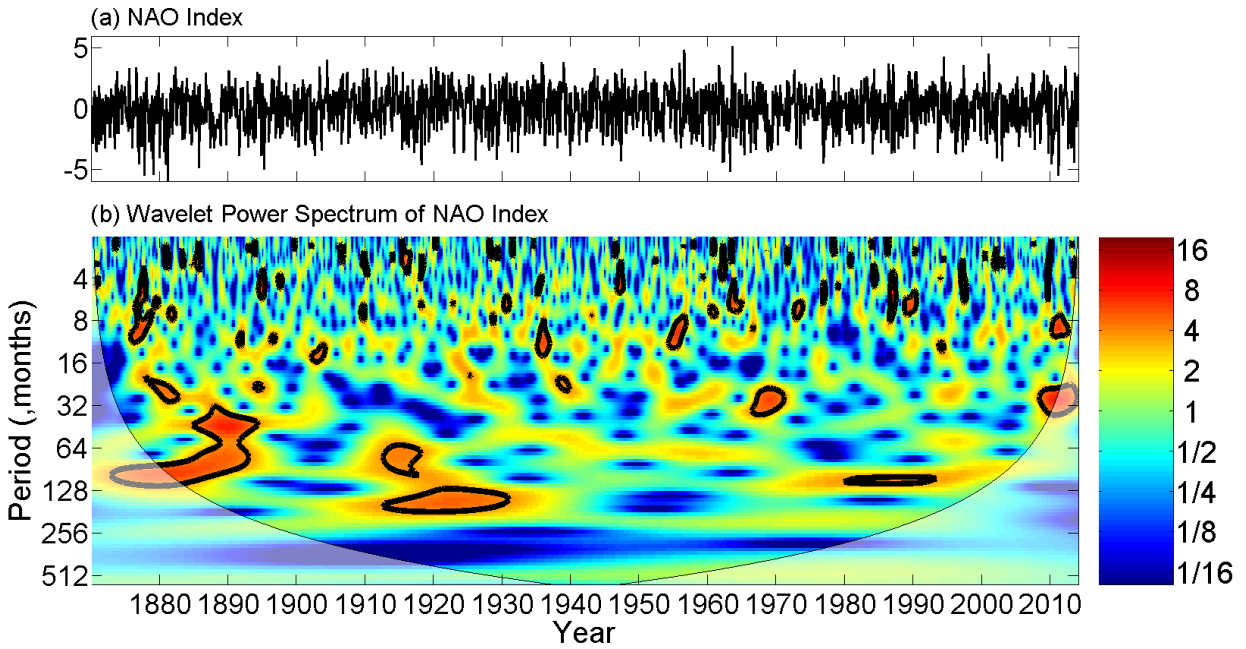
24 Hayes, M. H.: *Statistical Digital Signal Processing and Modeling*, John Wiley & Sons, New  
25 York, 624, 1996.

26 Hanna, E., Cropper, T. E., Jones, P. D., Scaife, A. A., and Allan, R.: Recent Seasonal Asymmetric  
27 Changes in the NAO (a Marked Summer Decline and Increased Winter variability) and Associated  
28 Changes in the AO and Greenland Blocking Index, *Int. J. Climatol.*, 2014.

29 Hurrell, J. W., Kushnir, Y., Ottersen, G., and Visbeck, M. (Eds.): *The North Atlantic Oscillation:*  
30 *Climatic Significance and Environmental Impact*. *Geophys. Monogr. Ser.*, 134, American  
31 *Geophysical Union*, 279 [pp.](#), 2003.

- 1 Jenkins, G. W., Watts, D. G.: Spectral Analysis and its Applications. Holden-Day, San  
2 Francisco, California, 541 pp., 1968.
- 3 Kay, S. M.: Modern Spectral Estimation: Theory and Application, Prentice Hall, Englewood  
4 Cliffs, NJ, 560 pp., 1988.
- 5 King, T.: Quantifying Nonlinearity and Geometry in Time Series of Climate. *Quat. Sci. Rev.*, 15,  
6 247–266, 1996.
- 7 Labat, D.: Wavelet Analysis of the Annual Discharge Records of the World’s Largest Rivers,  
8 *Adv. Water Resour.*, 31, 109-117, 2008.
- 9 Labat, D.: Cross Wavelet Analyses of Annual Continental Freshwater Discharge and Selected  
10 Climate Indices, *J. Hydrol.*, 385, 269-278, 2010.
- 11 Latif, M., Keenlyside, N. S.: El Nino/Southern Oscillation Response to Global Warming, *Proc.*  
12 *Natl. Acad. Sci. USA*, 106, 20578–20583, 2008.
- 13 Lee, Y. J. and Lwiza, K. M. M.: Factors Driving Bottom Salinity Variability in the Chesapeake  
14 Bay. *Cont. Shelf Res.*, 28, 1352-1362, 2008.
- 15 Maraun, D. and Kurths, J.: Cross Wavelet Analysis: Significance Testing and Pitfalls, *Nonlin.*  
16 *Processes Geophys.*, 11, 505-514, 2004.
- 17 Maraun, D., Kurths, J., and Holschneider, M.: Nonstationary Gaussian Processes in Wavelet  
18 Domain: Synthesis, Estimation, and Significance Testing, *Phys. Rev. E*, 75, doi:  
19 10.1103/PhysRevE.75.016707, 2007.
- 20 Meyers, S. D., Kelly, B. G., and O’Brien, J. J.: An Introduction to Wavelet Analysis in  
21 Oceanography and Meteorology: With Application to the Dispersion of Yanai Waves. *Mon.*  
22 *Weather Rev.*, 121, 2858–2866, 1993.
- 23 Müller, W. A., Frankignoul, C., and Chouaib, N.: Observed Decadal Tropical Pacific–North  
24 Atlantic Teleconnections. *Geophys. Res. Lett.*, 35, doi:10.1029/2008GL035901, 2008.
- 25 Ng, E. K.W. and Chan, J. C. L.: Geophysical Applications of Partial Wavelet Coherence and  
26 Multiple Wavelet Coherence. *J. Atmos. Oceanic Technol.*, 29, 1845–1853, 2012.
- 27 Özger, M., Mishra, A. K., and Singh, V. P.: Low Frequency Drought Variability Associated with  
28 Climate Indices. *J. Hydrol.*, 364, 152–162, 2009.
- 29 Paluš, M. and Novotná, D.: Quasi-biennial Oscillations Extracted from the Monthly NAO Index  
30 and Temperature Records are Phase-synchronized. *Nonlin. Process. Geophys.*, 13, 287–296,  
31 2006.

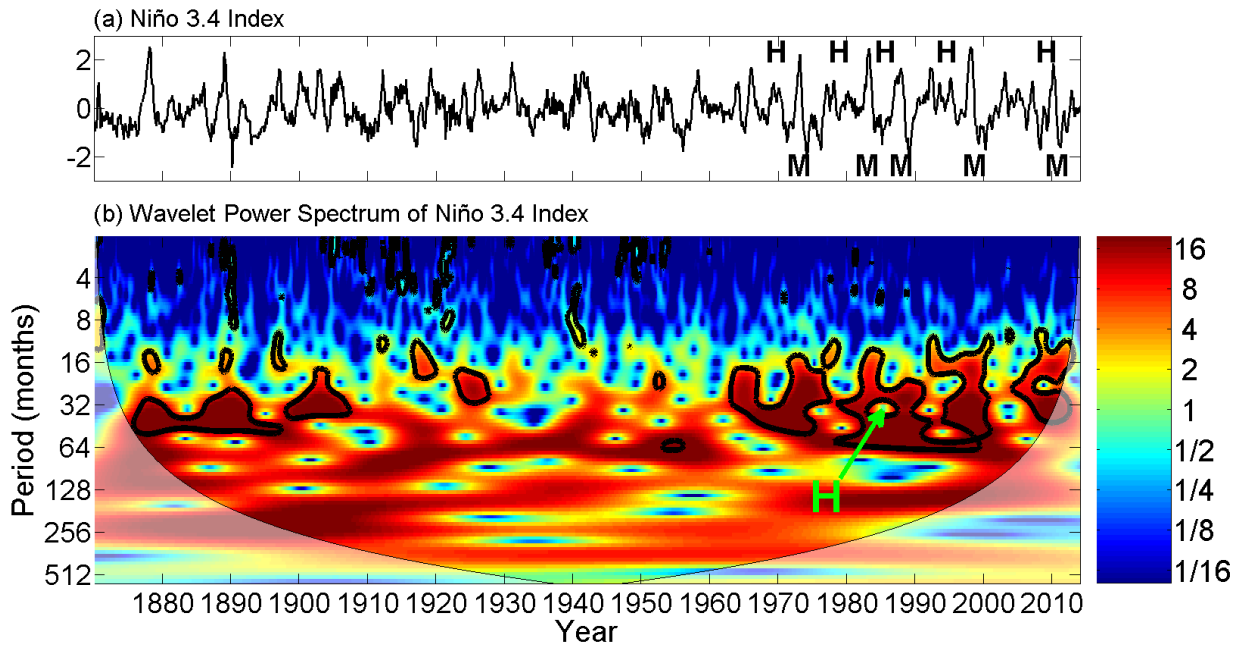
- 1 Schimanke, S., Körper, J., Spangehl, T., and Cubasch, U.: Multi-decadal Variability of Sudden  
2 Stratospheric Warmings in an AOGCM. *Geophys. Res. Lett.*, 38, doi: 10.1029/2010GL045756,  
3 2011.
- 4 Terradellas, E., Soler, M. R., Ferreres, E., and Bravo, M.: Analysis of Oscillations in the Stable  
5 Atmospheric Boundary Layer Using Wavelet Methods. *Boundary-Layer Meteorol.*, 114, 489–  
6 518, 2005.
- 7 Torrence, C. and Compo, G. P.: A Practical Guide to Wavelet Analysis, *Bull. Am. Meteorol.*  
8 *Soc.*, 79, 61–78, 1998.
- 9 Trenberth, K. E.: The Definition of El Niño, *Bull. Amer. Meteor. Soc.*, 78, 2771-2777, 1997.
- 10 Tropea, C., Yarin, A. L., and Foss, J. F. (Eds.): *Springer Handbook of Experimental Fluid*  
11 *Mechanics*. Springer, Berlin, Germany, 1557, 2007.
- 12 Velasco, V. M. and Mendoza B.: Assessing the Relationship between Solar Activity and Some  
13 Large Scale Climatic Phenomena, *Adv. Sp. Res.*, 42, 866–878, 2008.
- 14 Wilks, D. S.: On “Field Significance” and the False Discovery Rate, *J. Appl. Meteor. Climatol.*,  
15 45, 1181-1189, 2006.
- 16 Worsby, F. M., Duckham, M.: *GIS: A Computing Perspective*, CRC Press, Boca Raton, FL, 448  
17 [pp.](#), 2004.
- 18 Zhang, Q., Xu, C., Jiang, T., and Wu, Y.: Possible Influence of ENSO on Annual Maximum  
19 Streamflow of the Yangtze River, China, *J. Hydrol.*, 333, 265–274, 2007.
- 20 Ziegler, G. M.: *Lectures On Polytopes*, Graduate Texts in Mathematics, 152 [pp.](#), Springer, New  
21 York, 370, 1995.



1

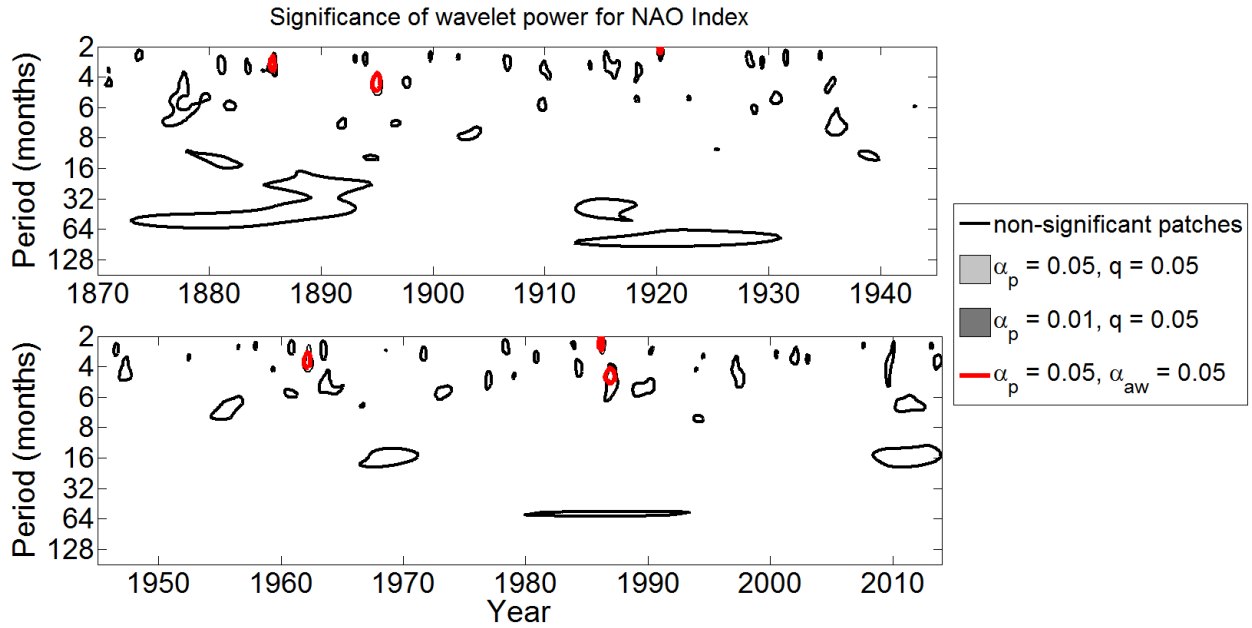
2 Figure 1. (a) The NAO index from 1870 to 2013. (b) The normalized wavelet power spectrum of  
 3 the NAO index. Thick contours enclose regions of 5% pointwise significance. Light shading  
 4 corresponds to the cone of influence, the region in which edge effects become important.

5



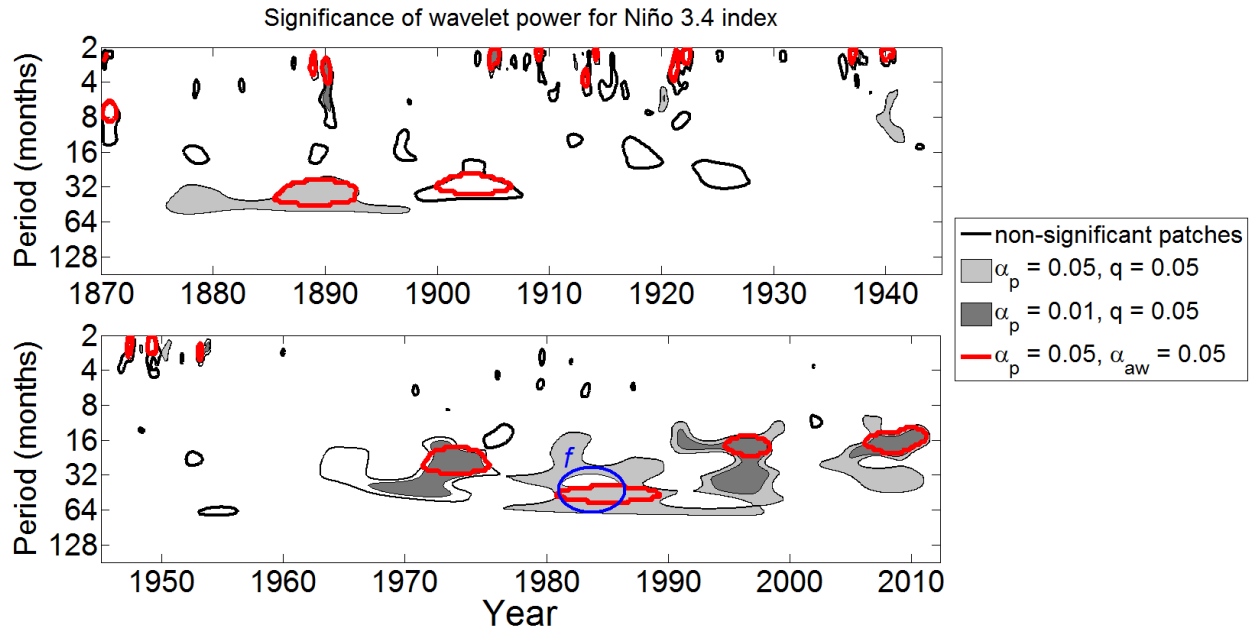
1

2 Figure 2. (a) The Niño 3.4 index time series from 1870 to 2013. Points labeled *M* indicate where  
 3 the merging process occurred and points labeled *H* indicate where a hole was formed (see Sect.  
 4 5.2 for details). (b) Same as Fig. 1b except for the Niño 3.4 index for the period 1870-2013. *H*  
 5 together with the arrow marks the location of a hole.

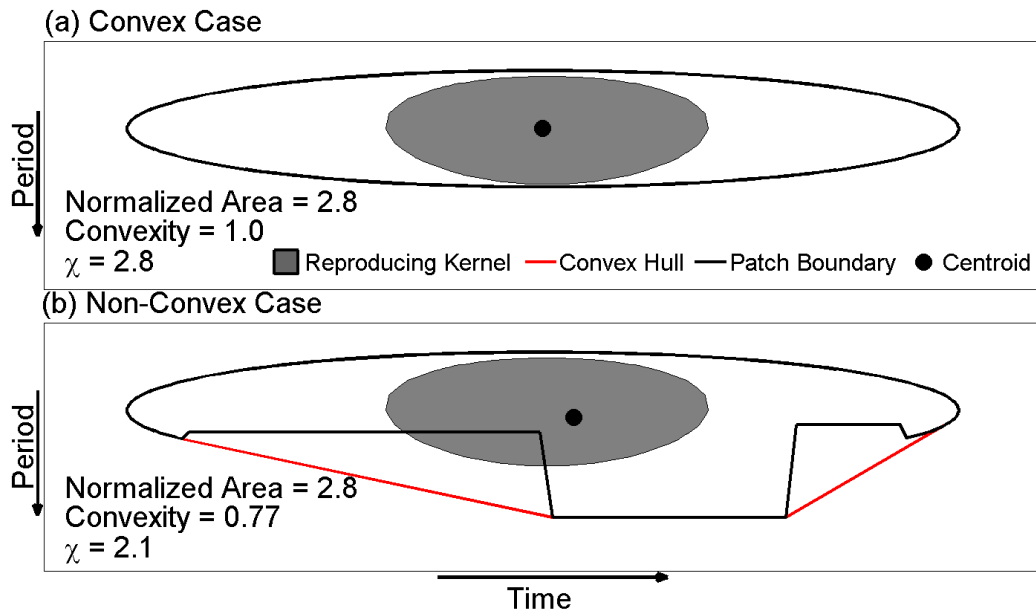


1

2 Figure 3. Significance of wavelet power for the NAO index mean monthly values for the period  
 3 1870-2013. Black contours enclose regions of 5% pointwise significance (see Sect. 3.1) and thick  
 4 red contours are the 5% areawise-significant subsets (see Sect. 3.2). Light gray shading indicates  
 5 those 5% pointwise significance patches that are geometrically significant at the  $q = 0.05$  level and  
 6 dark gray shading indicates those 1% pointwise significance patches that are geometrically  
 7 significant at the  $q = 0.05$  level.

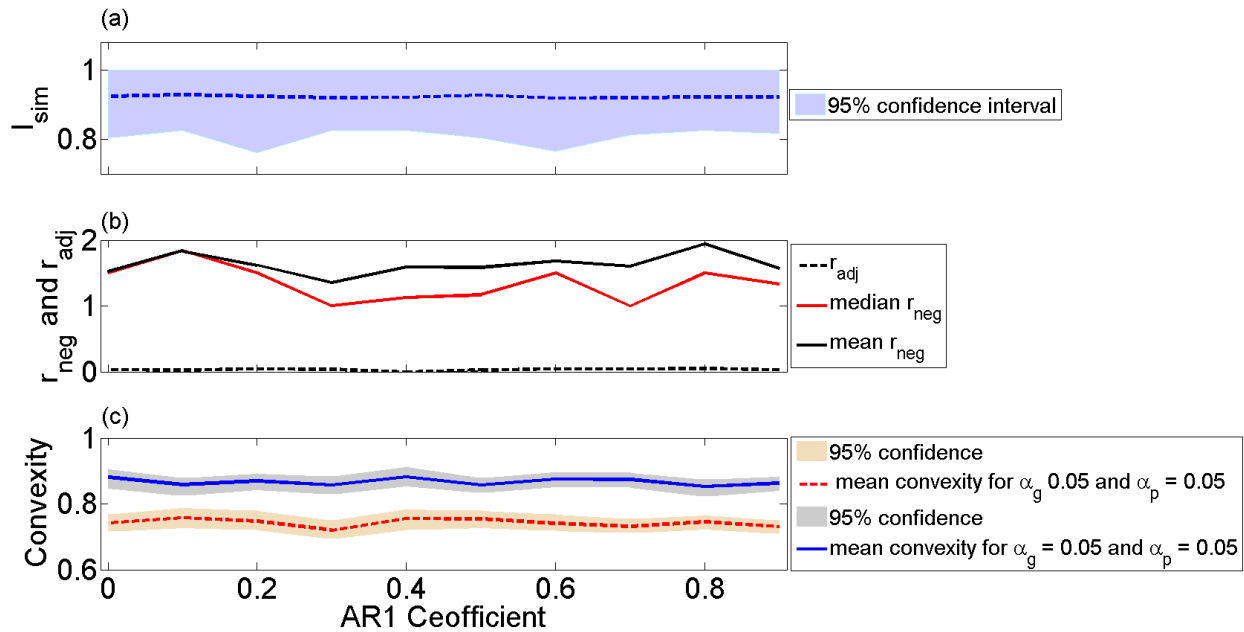


1  
 2 Figure 4. Same as Fig. 3 but for the Niño 3.4 for the period 1870-2013. The blue curve represents  
 3 a closed path  $f$  that is not contractible to a point because it surrounds a hole (see Sect. 5.1 and Fig.  
 4 2).

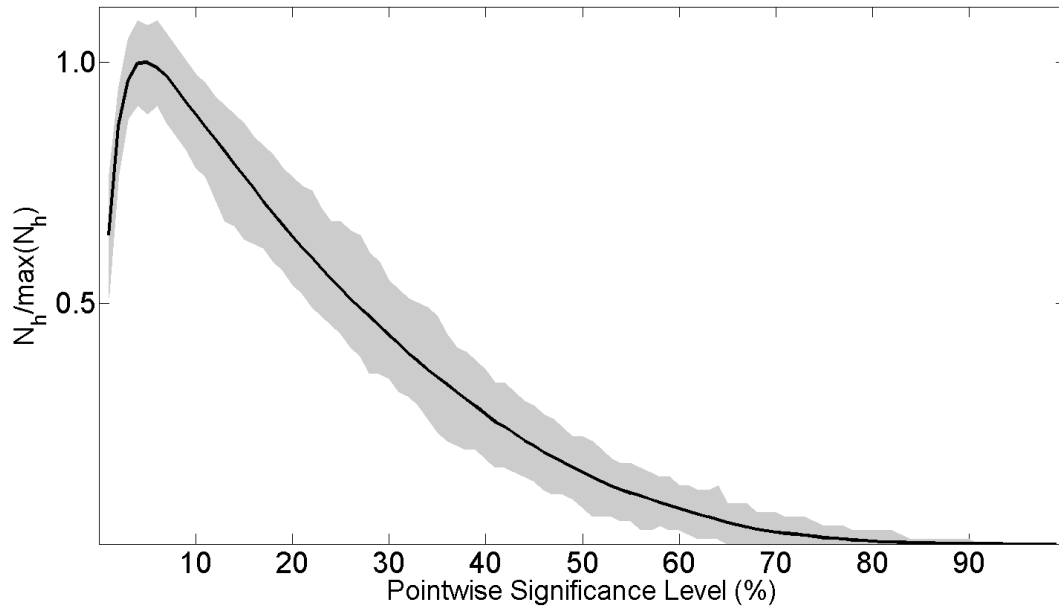


1  
2 Figure 5. (a) An idealized convex pointwise significance patch whose boundary is indicated by the  
3 black contour and whose centroid is indicated by the black dot. For reference, the reproducing  
4 kernel associated with the areawise test is shown, which is indicated by gray shading. In this case,  
5 the reproducing kernel lies entirely inside the patch. The convexity, normalized area, and  $\chi$  are  
6 displayed on the bottom left corner. (b) Same as (a) except the area of the convex hull (red curve)  
7 is not equal to the area of the patch and the reproducing kernel is unable to fit entirely inside the  
8 patch.



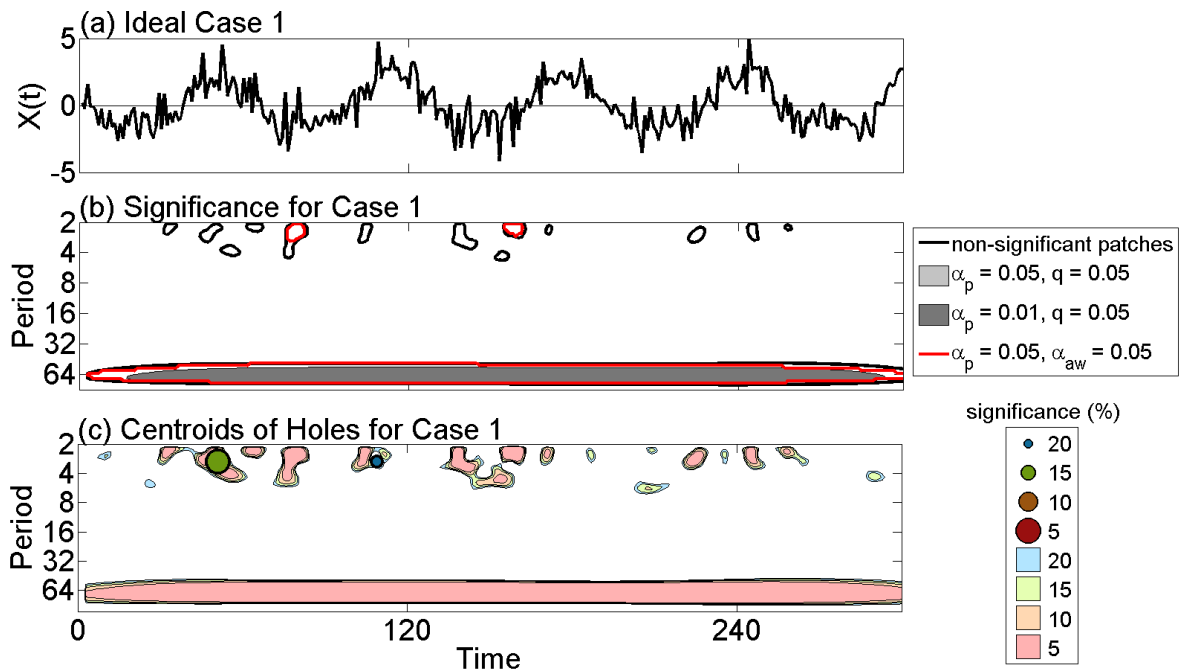


1  
 2 Figure 6. (a) Similarity index between the geometric and areawise tests for different lag-1  
 3 autocorrelation coefficients for red-noise processes (see text). (b) Same as (a) except for the ratio  
 4 between the false positive results of the geometric and areawise tests. The dotted black line  
 5 represents the ratio of false positive between the two tests when the false discovery rate of the  
 6 geometric test is controlled at the 0.05 level. (c) Same as (a) but for the mean convexity of 5%  
 7 pointwise significance patches that are geometrically significant at the 5% level and for the mean  
 8 convexity of 5% pointwise significance patches that are areawise significant at the 5% level.



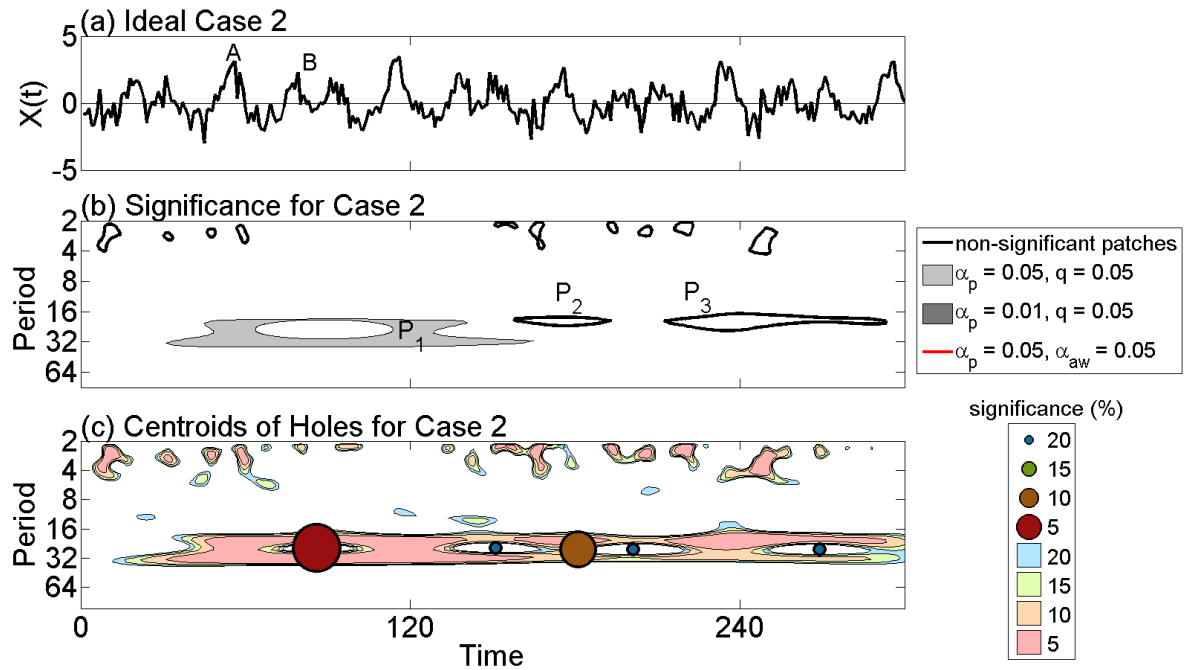
1  
2 Figure 7. Normalized mean number of holes as a function of pointwise significance level. The  
3 number of holes was calculated by generating 10,000 synthetic wavelet power spectra of red-noise  
4 processes with fixed autocorrelation coefficients of 0.5 and computing the number of holes Gray  
5 shading represents the 95% confidence interval.

6



1 Figure 8. (a) Time series of Case 1, which results from passing a single sinusoidal input with period  
 2  $\lambda = 64$  through Eq. (16). Gaussian additive white noise with a signal-to-noise of 2 was added to  
 3 the output response. (b) The significance of wavelet power for Case 1 (see Fig. 3 for details). (c)  
 4 Topological wavelet diagram corresponding to (b). Points are the centroids of the holes at a given  
 5 pointwise significance level, where both the color and size of the dots indicate the pointwise  
 6 significance level at which the hole existed. The shading of the patches corresponds to the  
 7 pointwise significance level at which the wavelet power coefficient existed, with the color of the  
 8 shading lighter than the dots for clarity.

9

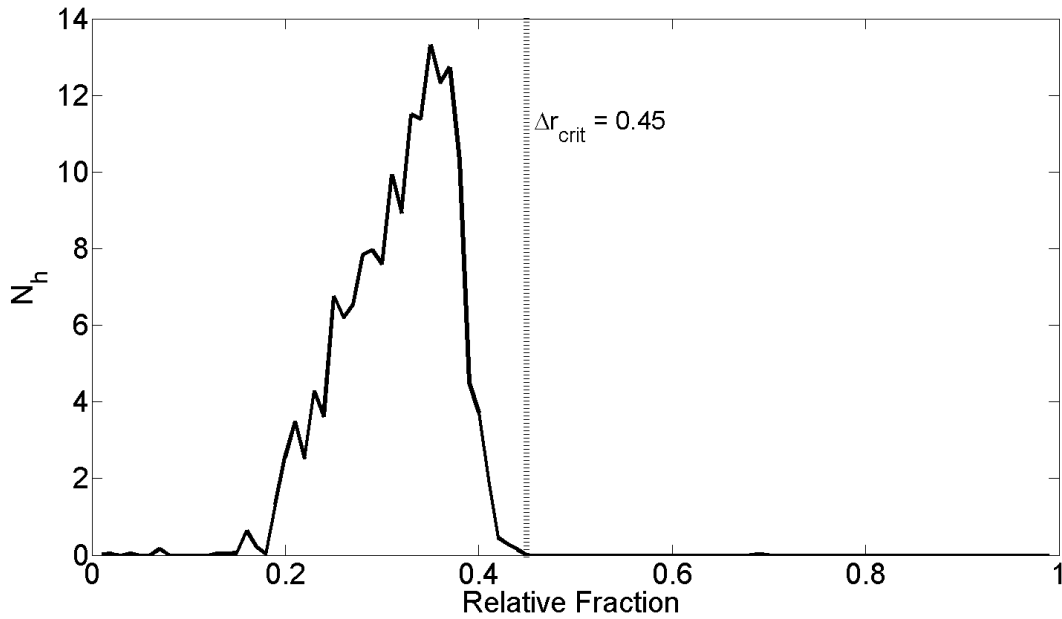


1

2 Figure 9. (a) Time series of Case 2. Gaussian additive white noise with a signal-to-noise ratio of 8  
 3 was added to the time series. At the point labeled A, two oscillations resonate, merging two  
 4 pointwise significance patches in the wavelet domain. At the point labeled B no such resonance  
 5 occurs and the two significance patches separate. (b) The significance of wavelet power (see Fig.  
 6 3 for details). The pointwise significance patch labeled  $P_1$  contains a hole and the pointwise  
 7 significance patches labeled  $P_2$  and  $P_3$  were falsely deemed insignificant by the geometric and  
 8 areawise tests. (c) Same as Fig. 8c except for Case 2.

9

1

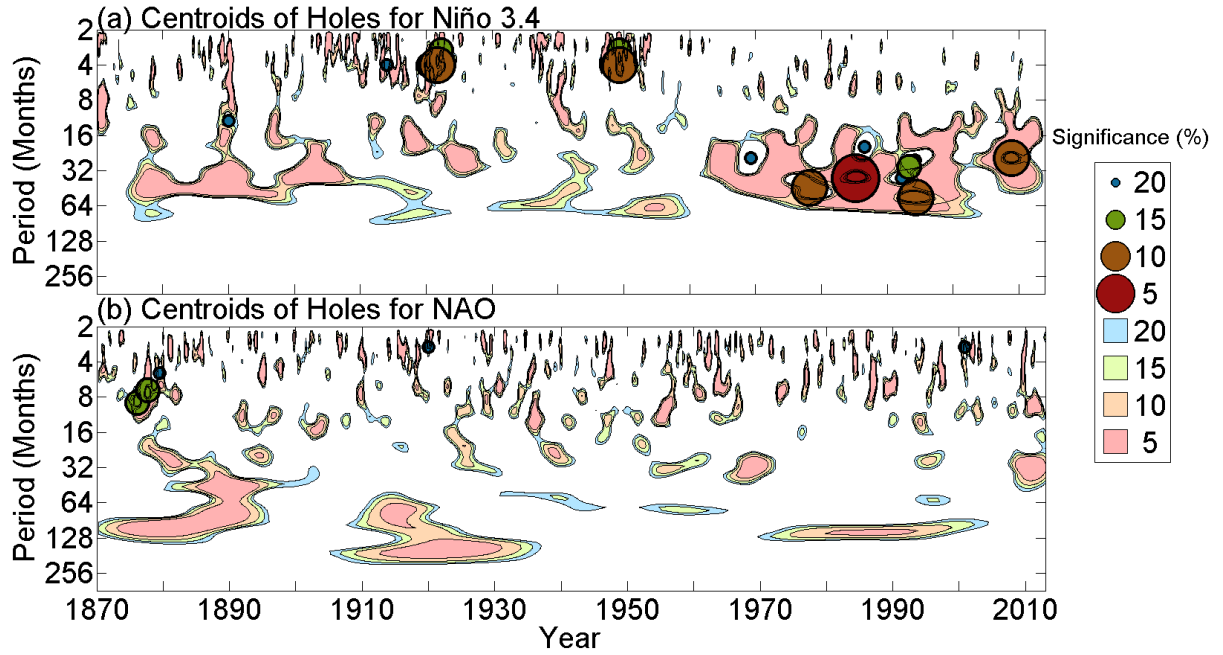


2

3 Figure 10. Mean number of holes found in 5% pointwise significance patches as a function of  
4  $\Delta r = (f_2 - f_1) / f_2$  for a sum of two sinusoids with amplitudes equal to unity and frequency  
5 components  $f_1$  and  $f_2$  such that  $f_2 > f_1 > 0$ . Additive white noise with a signal-to-noise ratio of 30  
6 was added to the sum of sinusoids. Pointwise significance was tested against a red-noise  
7 background. Dashed line represents the critical value of  $\Delta r$ , the value beyond which holes will  
8 rarely occur between oscillations of equal amplitude (set to unity) with frequencies  $f_1$  and  $f_2$ .

9

10



1

2 Figure 11. Same as Fig. 8c but for the mean monthly (a) Niño 3.4 and (b) NAO index anomalies  
 3 for 1870-2013.

- 1 Table 1. Fraction of pointwise significance patches containing at least  $N_h$  holes as a function of
- 2 the pointwise significance level calculated from an ensemble of 200,000 significance patches
- 3 generated from red-noise processes with fixed autocorrelation coefficients equal to 0.5.

Significance level (%)	$N_h \geq 1$	$N_h \geq 2$	$N_h \geq 3$	$N_h \geq 4$
<b>20</b>	$2.3 \times 10^{-2}$	$2.6 \times 10^{-3}$	$4.0 \times 10^{-3}$	0
<b>15</b>	$1.0 \times 10^{-2}$	$5.0 \times 10^{-3}$	$1.0 \times 10^{-3}$	0
<b>10</b>	$2.0 \times 10^{-3}$	$1.0 \times 10^{-3}$	0	0
<b>5</b>	$3.4 \times 10^{-4}$	0	0	0
<b>1</b>	0	0	0	0